Journal of Loss Prevention in the Process Industries 40 (2016) 507–523

Contents lists available at ScienceDirect

Journal of Loss Prevention in the Process Industries

journal homepage: www.elsevier.com/locate/jlp

A review on understanding explosions from methane–air mixture

Sazal Kundu, Jafar Zanganeh*, Behdad Moghtaderi

Priority Research Centre for Frontier Energy Technologies & Utilisation, Discipline of Chemical Engineering, School of Engineering, Faculty of Engineering & Built Environment, The University of Newcastle, Callaghan, NSW 2308, Australia

ARTICLE INFO

Article history:
Received 24 November 2015
Received in revised form
1 February 2016
Accepted 1 February 2016
Available online 8 February 2016

Keywords:
Mine safety
Methane–air based explosion
Flame acceleration
Deflagration to detonation transition
Obstacles for flame acceleration
Confinement on flame acceleration

ABSTRACT

This review examines existing knowledge on the genesis and flame acceleration of explosions from methane–air mixtures. Explosion phases including deflagration and detonation and the transition from deflagration to detonation have been discussed. The influence of various obstacles and geometries on explosions in an underground mine and duct have been examined. The discussion, presented here, leads the readers to understand the considerations which must be accounted for in order to obviate and/or mitigate any accidental explosion originating from methane–air systems.

1. Introduction

Methane– air systems are life-threatening mixtures particularly in underground coal mines. Explosions initiated by these mixtures have destroyed infrastructure in the mines and taken thousands of lives in the past. The explosion which occurred in Mount Kembla Mine in 1902 was the worst mining tragedy in Australian history, killing 96 people (Radford, 2014). The second worst disaster, according to the lives lost, occurred earlier in 1887 which took the lives of 81 miners from the Bulli Mine (Brown, 2010; Dingsdag, 1993). Methane from coal mines initiated explosions in these disasters and the explosions are later escalated by coal dust. The deadliest coal mine explosion in human history occurred in 1942 at the Benxihu Colliery, China killing 1549 people (Dhillon, 2010a). A number of other coal mine explosions are reported in literature (Dhillon, 2010a,b; Tu, 2011). In each explosion disaster, lives were lost and resulted in immense financial loss to the mining companies. The severity of these disasters motivated a number of researchers to initiate research on methane–air systems.

Explosions cannot be initiated for every concentration of combustible gas in air. The concentration range of a combustible gas for which explosions can originate is known as explosion limit/range or flammability limit/range. While a combustible-air mixture within the flammability range can develop into explosion, such explosions may be deflagration, detonation or may transit from deflagration to detonation. When the combustion wave propagates at a speed lower than the speed of sound, the explosion is termed deflagration (Fig. 1) (Suzuki et al., 2005). The temperature of combustion products is much higher than room temperature. As the speed of sound increases with increasing temperature, the explosion sound, travelling in combustion products becomes very high. As a consequence, the limit of deflagrated flame speed for combustion products is much higher than the speed of sound in air at room temperature. In contrast, a combustion wave that propagates much faster than the speed of sound at the specific temperature is termed detonation. The pressure rise in detonation is much higher than deflagration and can be calculated by correlations for the Chapman-Jouguet condition (Chapman, 1899; Jouguet, 1905). Mathematically, detonation refers to the pressure and flame speeds equal to and higher than those estimated by Chapman-Jouguet correlations. Compared to original pressure, the pressure may rise up to eight times in deflagration (King, 1990). In detonation, the peak pressure may reach twenty times or more (James; King, 1990). In addition, shock waves generated in detonation are very ruinous (King, 1990). Briefly, detonation is much more detrimental

Abbreviations: DDT, deflagration to detonation transition; LEL, lower explosive limit; LFL, lower flammability limit; UEL, upper explosive limit; UFL, upper flammability limit; BR, blockage ratio; CJ, Chapman-Jouguet; LPG, liquefied petroleum gas; *L/D*, length-to-diameter ratio.

* Corresponding author.
E-mail address: Jafar.Zanganeh@newcastle.edu.au (J. Zanganeh).

http://dx.doi.org/10.1016/j.jlp.2016.02.004
0950-4230/

Nomenclature

Symbols

Φ	equivalence ratio of fuel (dimensionless)
M	Mach number (dimensionless)
ϕ	degree of confinement (dimensionless)
φ	width or height of a square cross-section of mine gallery (m)
λ	detonation cell size (cm)
P_f	pressure of hydrogen–oxygen mixture in the initiator tube (atm)
E_c	total chemical energy of the stoichiometric hydrogen –oxygen mixture per unit volume at atmospheric pressure (J m^{-3})
V_i	volume to the initiator tube (m^3)
Q_{H_2}	heat of combustion of hydrogen (J m^{-3})
d	orifice plate bore diameter (m)
D	inner diameter of the explosion tube (m)
L	length of the explosion tube (m)
A_o	the largest cross-sectional area blocked by an obstacle (m^2)
A_d	inner cross-sectional area of the explosion duct (m^2)
l	length of an obstacle bar (m)
x	diameter of the circular area for an cylindrical obstacle bar or a side for triangular or square obstacle bar (m)
E_g	generation of thermal energy due to combustion of the flammable gas (J)
E_l	loss of energy due to the sharp rise of local temperature to final flame temperature (J)
U_{obs}	measured flame speed (m s^{-1})
U_{cj}	flame speed at Chapman-Jouguet condition (m s^{-1})
C_f	wall drag coefficient (dimensionless)
R	radius of a tube (m)

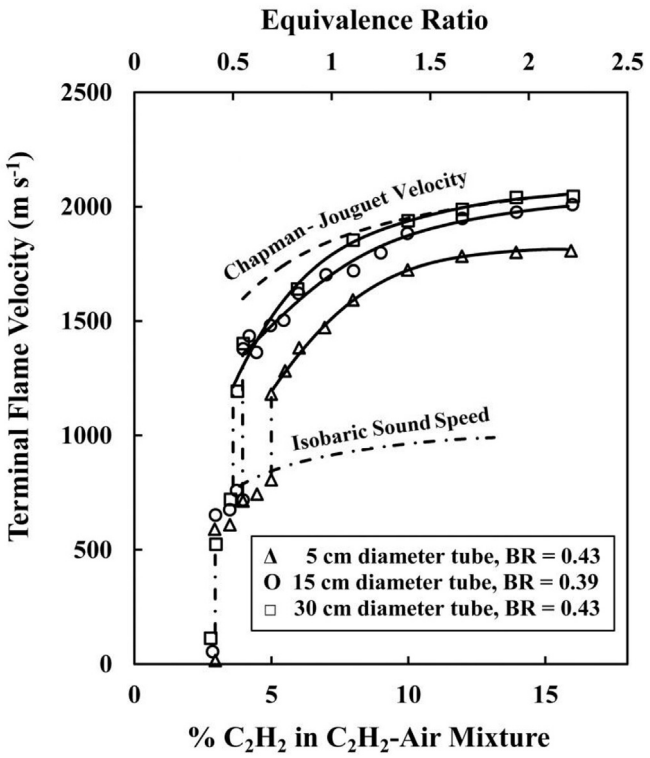

Figure 1. Illustration of deflagration and detonation limits as presented by isobaric speed of sound and speed at Chapman-Jouguet condition lines constructed from experiments conducted for the acetylene–air mixtures (Peraldi et al., 1986).

compared to deflagration.

Interestingly, there is no particular name for the flame of an explosion within the limits of isobaric sound speed and speed at Chapman-Jouguet condition (Fig. 1). However, explosions with flame velocities lower than but close to speed at Chapman-Jouguet condition are often termed as quasi-detonation. When a transition occurs for a low speed deflagrated flame, it reaches quasi-detonation or detonation. The phenomenon of the transformation of a low speed deflagrated flame to a catastrophic detonation explosion is known as Deflagration to Detonation Transition or DDT.

A deflagration flame transition to quasi-detonation or detonation was found to occur in the presence of a number of factors including obstacles and particular geometries of explosion galleries. The shapes of obstacles are important in accelerating flame propagation. Orifice plates and Shchelkin spirals are commonly employed obstacles in experimental investigations; however, the obstacles present in the real world are diverse. The geometries of explosion galleries, briefly confined, semi-confined and unconfined, are also important in flame acceleration. The analyses of various investigations found in literature are presented in this article with the aim of providing an understanding of explosions originating from methane–air systems.

2. Explosion limits of methane–air mixtures

When methane build-up in an underground coal mine reaches a certain concentration range, explosion can be initiated by the presence of a small heat source. The minimum concentration of methane (in air) of this explosive concentration range is its Lower Flammability Limit (LFL) or Lower Explosive Limit (LEL). In contrast, the maximum concentration of this range is the Upper Flammability Limit (UFL) or Upper Explosive Limit (UEL) of methane in air (Gharagheizi, 2008). When methane concentration falls below LEL, the amount of methane becomes too low to ignite. Similarly, the amount of oxygen becomes too low when the methane concentration reaches above UEL and no ignition occurs. The LEL is limited by the fuel source (methane concentration) while the UEL is limited by the oxidant (oxygen concentration).

Several researchers investigated the flammability range of methane (Bartknecht, 1993; Bunev et al., 2013; Checkel et al., 1995; Chen et al., 2011; Claessen et al., 1986; Gieras et al., 2006; Vanderstraeten et al., 1997). The outcome of these researches concludes that the LEL of methane is 4.6 ± 0.3% (the concentrations presented in this article are in volume basis) while the UEL of methane is 15.8 ± 0.4% when methane is ignited in air at 20 °C and 100 kPa (relates to ambient temperature and pressure) as presented in Fig. 2 (Vanderstraeten et al., 1997). In addition, the maximum pressure rise occurs at a methane concentration of ~9.5%.

The explosion parameters depend largely on initial temperature and pressure. As can be seen in Fig. 3, the UEL value of methane increases, shifts towards the right, at elevated initial pressures. In addition, a couple of zones are observed for methane–air mixture

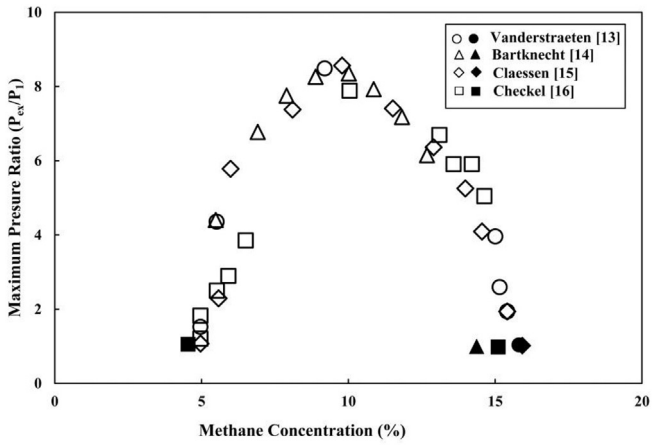

Fig. 2. LEL, UEL and maximum explosion pressure ratios for methane–air mixtures ignited at 20 °C and 100 kPa (open marker – successful, covered marker – unsuccessful) (Vanderstraeten et al., 1997).

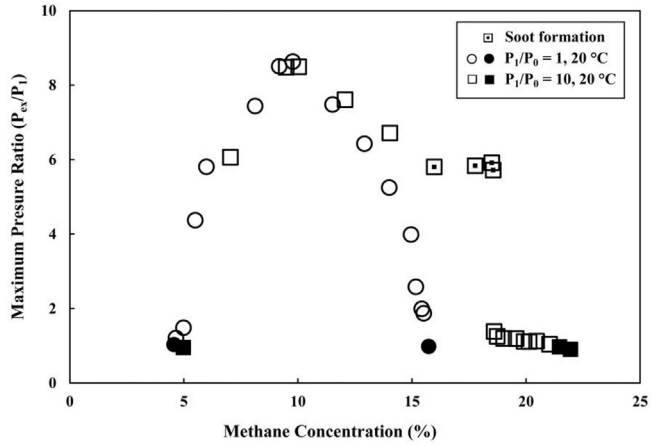

Fig. 3. Effect of initial pressure on the explosion pressure rise for methane–air mixtures ignited at 20 °C and at 100 kPa and 1000 kPa (open marker – successful, covered marker – unsuccessful) (Vanderstraeten et al., 1997).

at elevated pressures, known as the soot zone and the twilight zone (Goethals et al., 1999; Vanderstraeten et al., 1997). The explosion pressure to initial pressure ratio plateaus at the soot zone. As presented in Fig. 3, a soot zone was found for methane–air mixtures with methane concentrations between 16.0 and 18.6%. When the explosion pressure to initial pressure ratio is very low, usually less than 2, the twilight zone appears. As illustrated in Fig. 3, the twilight-zone for methane–air mixtures develops at a methane concentration of 18.7% where the pressure ratio is 1.5. The pressure ratio drops to unity at a methane concentration of 21.7%, which is the end point of the twilight-zone (Vanderstraeten et al., 1997).

The initial temperature has a tremendous effect on explosion parameters. At higher temperatures, the UEL value of methane increases while the LEL decreases (Fig. 4) (Gieras et al., 2006). More importantly, the explosion pressure reduces with the increase of initial temperature. At elevated temperature, the reaction rates are higher. However, the total mass of the combustible gas in the combustible-air mixture is lower at elevated temperatures when compared to that at reduced temperatures maintaining constant initial pressure. The faster reaction rate at elevated temperature drives the explosion towards higher pressure while the lower amount of combustible gas leads the explosion towards lower

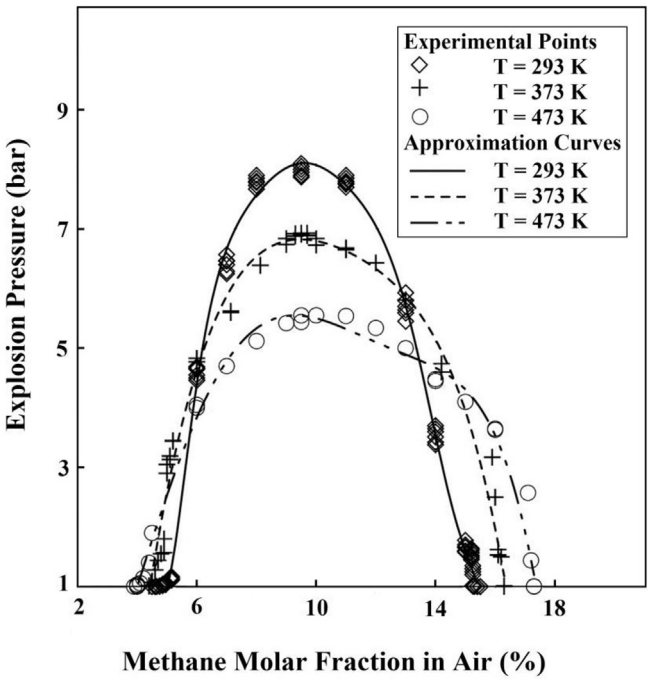

Fig. 4. Effect of initial temperature on explosion pressure rise for methane–air mixtures (Gieras et al., 2006).

pressure. The overall effect results in lower explosion pressures at elevated temperature.

The discussion presented here leads to the conclusion that the concentration of methane is the very important explosion parameter. All of these investigations revealed that a methane concentration of ~9.5% in air is the most explosive methane–air mixture. While any methane concentration within the flammability range has the potential to explode in the presence of an ignition source, a methane concentration of ~9.5% in air can produce the most damaging explosion.

Methane gas, trapped in the coal matrix during coalification process, is released when coal is mined (Thakur, 2006). The released gas may accumulate in various places of coal mines and become a potential hazard for explosion. Depending on the amount of methane released and the level of available ventilation, the concentration of accumulated methane may vary widely. It is possible that the concentration of accumulated methane reaches 9.5% in some areas of coal mines. Investigations on the accidents of Mount Kembla Mine, Bulli Mine of Australia and Benxihu Colliery Mine of China revealed that methane gas played a key role in explosions of these accidents (Dhillon, 2010b). Although it is hard to anticipate what level of methane concentration was reached in these explosions, it can be predicted that the concentration of methane in these accidents was within the flammability limits of methane.

3. Ignition pathways of a flammable mixture

3.1. Auto-ignition

When the concentration of a flammable substance in a combustible – oxidant system is within the flammability range, ignition can occur in two ways. One of these pathways is known as auto-ignition. In this ignition process, the flammable substance ignites spontaneously without any ignition source (e.g., flame or spark) at or above a certain temperature. The lowest temperature at which the spontaneous ignition occurs is known as auto-ignition

temperature or kindling point (Pan et al., 2008; Robinson and Smith, 1984).

A comparison of auto-ignition temperatures derived by various researchers are presented in Table 1 (extracted from (Robinson and Smith, 1984)).

A number of researchers worked with the aim of determining minimum auto-ignition temperature dependent on the concentration of methane in air. The auto-ignition temperature of methane in air was reported as 537 °C (999 °F) in (AFMFI, 1940) while the majority of reported literature values were higher than 600 °C (Bunte and Bloch, 1935; Coward, 1934; Fenstermaker, 1982; Freyer and Meyer, 1893; Naylor and Wheeler, 1931; Robinson and Smith, 1984; Taffenel, 1913; Townend and Chamberlain, 1936).

Robinson et al. found the minimum auto-ignition temperature at a methane concentration of 7%. While the minimum auto-ignition temperature of methane was found to be different in the study of Naylor et al., they also found their minimum auto-ignition temperature at a methane concentration of 7%. Results from Naylor et al. and Robinson et al. are presented in Fig. 5 (extracted from (Robinson and Smith, 1984)).

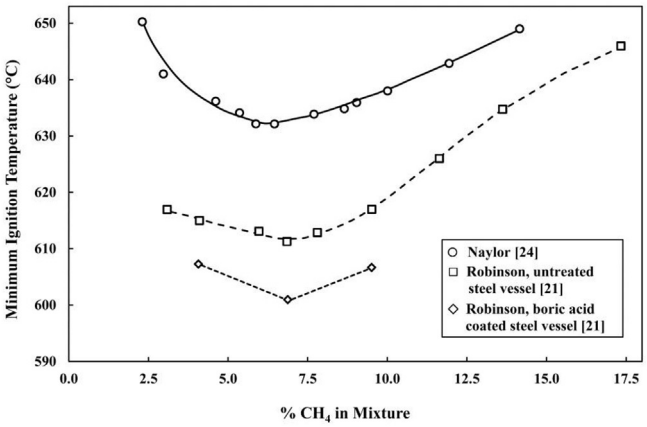

Fig. 5. Outcomes of experiments in the determination of auto-ignition temperature for methane in air (Robinson and Smith, 1984).

3.2. External ignition source

When the combustible-air mixture is at lower temperature than the minimum auto-ignition temperature, an alternative pathway is required to initiate ignition. In this ignition process, an external ignition source such as flame or spark is employed (Kuchta, 1985). For a particular type of external ignition source, higher ignition energy results in a more devastative explosion (Ajrash et al., 2016a,b).

Fig. 6 represents spatial and temporal characteristics of various ignition sources. Although heated vessels have potentials to initiate combustion, they are large in size while their heating rate and temperature are relatively low. In contrast, sources that generate electric sparks are very small in size while their heating rate and temperature are high.

Ignition energies based on capacitive electric spark for various alkane-air mixture can be found in Fig. 7 (Eckhoff, 2005).

Methane has very low minimum ignition energy of 0.3 mJ when an electric spark is employed. The spark temperature greatly exceeds the methane minimum ignition temperature and the higher temperature of the spark helps in initiating ignition at very low ignition energy (Marinović, 1990).

In Fig. 7, the ignition energies are plotted against equivalence ratio of fuel (Φ). The term, equivalence ratio, is often used in literature. It is the ratio of the actual fuel–air ratio to the stoichiometric fuel–air ratio (Khanna, 2001).

$$\Phi = \frac{\left(\frac{Fuel}{Oxident}\right)_{actual}}{\left(\frac{Fuel}{Oxident}\right)_{stoichiometric}}$$

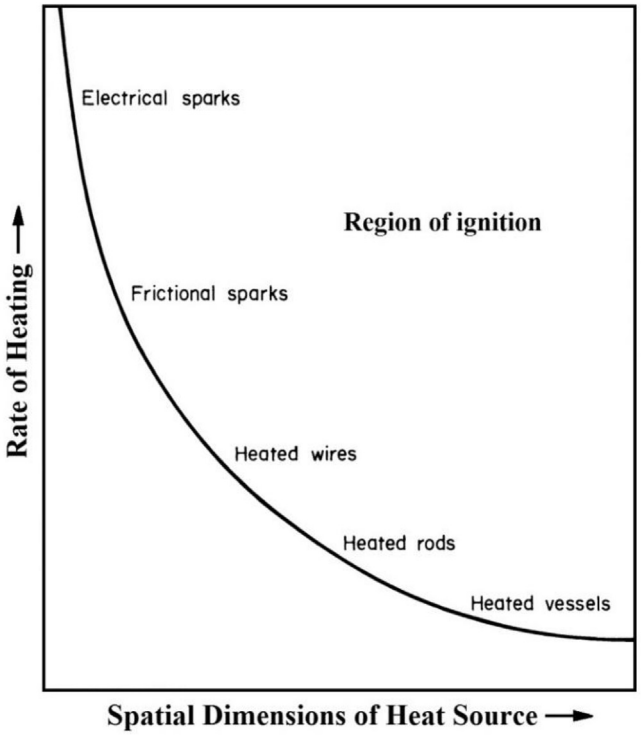

Fig. 6. Illustration of temporal and spatial characterisation of various ignition sources (Cheremisinoff, 2013; Kuchta, 1985).

The equivalence ratio plays an important role in combustion study (Andersson et al., 2003). When Φ = 1.0, the mixture is of

Table 1
Auto-ignition temperatures of methane in air determined experimentally in various studies.

Auto-ignition temperature (°C)	Ignition vessel	Reference
601	0.8 dm^3 steel sphere	(Robinson and Smith, 1984)
606–650	0.24 dm^3 glass cylinder	(Freyer and Meyer, 1893)
632	0.44 dm^3 quartz cylinder	(Naylor and Wheeler, 1931)
656	Ceramic tubing, volume not known	(Coward, 1934)
659	0.2 dm^3 steel sphere	(Fenstermaker, 1982)
673	0.19 dm^3 silica cylinder	(Townend and Chamberlain, 1936)
675	0.275 dm^3 glass cylinder	(Taffenel, 1913)
748	Steel tubing, diameter about 10 mm, length 165 mm	(Bunte and Bloch, 1935)

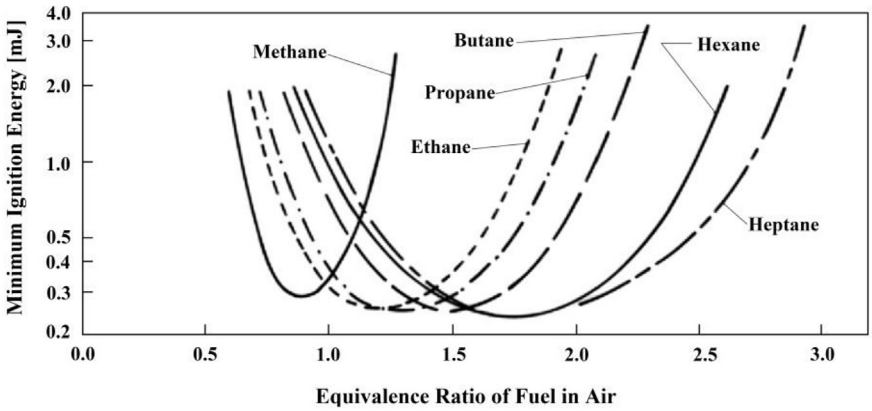

Fig. 7. The minimum ignition energies for alkane-air mixtures when capacitive electric sparks are employed (Eckhoff, 2005).

stoichiometric condition. When $\Phi < 1.0$, the mixture contains more oxidant than the stoichiometric value and the mixture is termed as a lean mixture. In contrast, when $\Phi > 1.0$, the mixture is a rich mixture as the mixture contains more fuel than the stoichiometric value.

Fig. 7, constructed for various fuel–air mixtures, represents minimum ignition energies estimated by capacitive sparks. In case of fuels like ethane, propane, butane, hexane and heptane, the minimum ignition energies were found for the rich mixtures of these fuels with air. In contrast, a lean-mixture of methane in air exhibited the minimum energy required for ignition for methane–air systems.

There are several other ways ignition can occur in addition to electric sparks or electric discharge (Kuchta, 1985). Common ignition sources include hot surfaces (e.g., heated vessels, heated wires, frictional sparks etc.), self-heating, hot gases and pyrophoric or hypergolic reactions (Ashman and Büchler, 1961; Eckhoff and Thomassen, 1994; Fitch, 1992; Kuchta, 1985).

Fig. 8 illustrates the generation of fire from a flammable substance in the presence of an ignition source.

At the point of ignition, a flammable substance ignites when exposed to an ignition source. In the next step, a critical volume of the flammable substance is required to be heated to produce an exothermic reaction that heightens flame beyond the ignition point (Fitch, 1992).

Initiation of ignition in coal mines is most common via external ignition sources rather than auto-ignition (Hartman et al., 2012). A number of ignition sources such as heat from diesel engines, static charge, sparks from shearing and spontaneous combustion of the coal face are present in underground mines (De Rosa, 2004). In both Mount Kembla Mine and Bulli Mine of Australia, the ignition source was naked flame (Lee, 2003; Organ, 1987). Sparks from damaged electrical equipment are dangerous and triggered one mine explosion in Bellbird Colliery Mine of Australia, which took the lives of 21 miners in 1923 (Markham, 1993). These accidents highlight that any potential source of ignition can cause devastative explosions in coal mines.

4. Effect of initiation energy on flame speed

The initiation energy (determined from the total chemical energy of the fuel in the initiator when employed) has tremendous effect on flame speed (Gamezo et al., 2012; Wolański et al., 1981). Wolański et al. investigated the variation of flame speed by changing initiation energy and methane concentration. They employed a square vertical tube of 6 m height and 63.5 mm width (the cross-section was approximately square in shape with rounded corners having a radius of curvature of 14.3 mm) (Wolański et al., 1981). In their experimental setup, a 1.12 m tube of 50 mm diameter, known as initiator tube, was obliquely connected with the

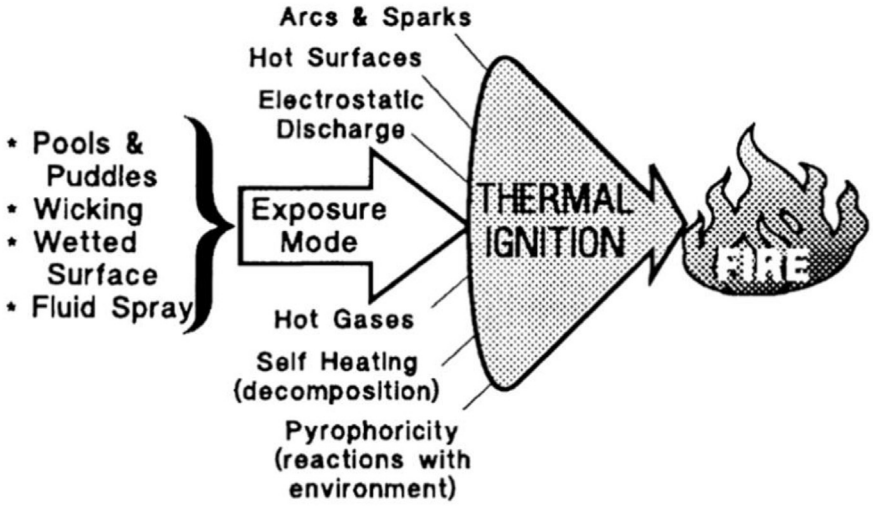

Fig. 8. Initiation of fire in the presence of various energy sources and fuel exposure modes (Fitch, 1992).

main tube. The initiator tube was isolated from the main tube by a Mylar diaphragm.

A stoichiometric hydrogen–oxygen mixture was employed in the initiator and a glow plug was used as a source of ignition. The initiation energy was determined from the initial pressure of hydrogen–oxygen mixture. The value of the initiation energy was obtained by estimating the total chemical energy in the initiator. The initiation energy per unit cross-sectional area, estimated by Wolański et al., may be expressed by $U = 0.5P_f E_c V_i/A_d$; where P_f is the pressure of hydrogen–oxygen mixture (in atm), E_c is the total chemical energy of the stoichiometric hydrogen–oxygen mixture per unit volume at atmospheric pressure, V_i is the volume to the initiator tube, A_d is the cross-sectional area of the main tube and the factor 0.5 is the fraction of hydrogen in the mixture at stoichiometric condition. If Q_{H_2} is the heat of combustion of hydrogen (in energy/volume unit), then the equation becomes, $U = 0.5P_f Q_{H_2} V_i/A_d$.

Wolański et al., expressed flame speed as Mach number (M), a dimensionless number which can be defined as follows (Perry and Kantrowitz, 1951):

$$M = \frac{speed\ of\ flame}{speed\ of\ sound\ in\ the\ undisturbed\ fluid\ ahead\ of\ the\ flame}$$

When the value of Mach number is more than one, the flame speed is supersonic. In contrast, the speed of flame is subsonic when the Mach number is less than one.

The investigation by Wolański et al. employing 28.2 MJ m^{-2} initiation energy revealed that the concentration of methane affects the final flame speed (Fig. 9). When the initiation energy was applied to methane–air mixtures constituted by 8, 9.5, 11 and 14.5% methane in air, they found that 11% methane in air produced the highest flame speed. From their extended investigations, they found a detonability limit of 8–14.5% for methane–air mixture, where a methane concentration of 12% in air provided the highest detonation velocity. While a stoichiometric ratio of methane–air mixture is expected to provide the highest detonation velocity, a shift towards higher concentrations of methane was found for this investigation. This is most likely due to the dilution of methane–air mixture by the combustion products of hydrogen–oxygen mixture from the initiator tube.

While investigating the impact of initiation energy on the flame speed, Wolański et al. introduced 5.8, 7.1, 8.3, 9.45 and 11.8 MJ m^{-2} initiation energy densities in their experiments (Fig. 10). The flame

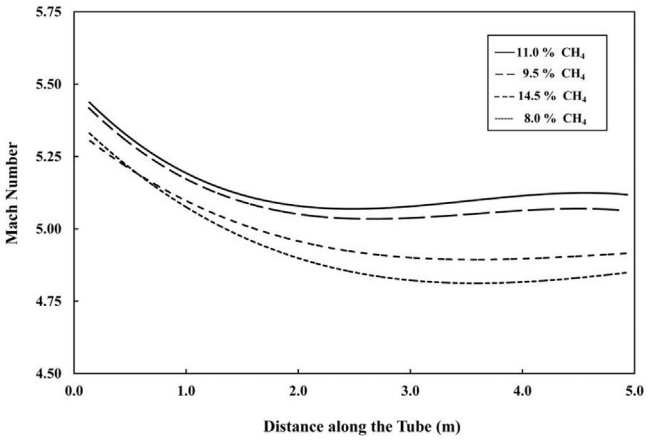

Fig. 9. Effect of initial concentration of combustible gas on the detonation velocity (extracted from the explosion studies of methane–air mixtures with an initiation energy of 28.2 MJ m^{-2}) (Wolański et al., 1981).

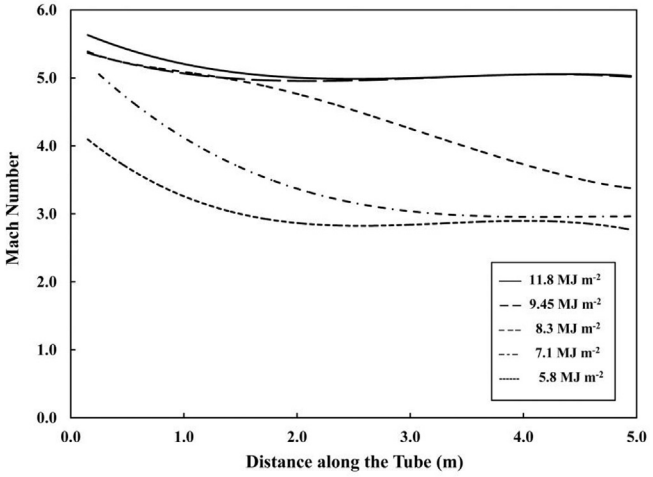

Fig. 10. Effect of initiation energies on the detonation velocity (extracted from explosion studies of methane–air mixtures with a methane concentration of 9.5% in air) (Wolański et al., 1981).

speed increased for the first four initiation energy densities; however, the changes in flame speed became almost unchanged from 9.45 to 11.8 MJ m^{-2}. This means that the flame speed increases up to a certain value of initiation energy. Above that value of initiation energy, the dependence of flame speed on initiation energy becomes negligible.

In coal mines, the volume and concentration of accumulated methane determines the total chemical energy present in the form of methane. If an explosion occurs, the initiation energy of this accumulated methane impacts on secondary coal dust explosions. The results and analyses of Wolański et al. provide an understanding of the effects of initiation energy on secondary explosions.

5. Effect of turbulence on explosion characteristics

In a combustion process, the flow becomes non-uniform in presence of obstacles leading towards the generation of turbulence in the flow. The burning speed, described as the rate at which a flammable gas mixture is consumed, increases with increasing turbulence in the flow field (Moen et al., 1980). The turbulence produced by obstacles sustains low speed flame (or deflagration) and transforms that low speed flame to high speed flame (detonation or quasi-detonation). In the real world, the types and nature of obstacles are diverse (Moen et al., 1980; Oran et al., 2015). Therefore, various types of obstacles, employed by researchers, provide an understanding of flame acceleration by obstacles for various fuel–air mixtures. This section includes discussion on a few types of obstacles employed in various researches with the aim of understanding explosion characteristics in the presence of turbulence created by those obstacles.

5.1. Shchelkin spiral

One of the effective obstacles in the studies of explosion characteristics is the Shchelkin spiral, developed by the physicist Kirill Ivanovich Shchelkin (Frolov, 2008; Frolov and Aksenov, 2007; Lu et al., 2005; Shchelkin and Troshin, 1964; Sorin et al., 2006; Takita and Niioka, 1996; Tsuboi et al., 2009). This obstacle was found to be very effective in sustaining deflagration and accelerating convertion to more destructive combustion waves in the explosion study of methane–air mixtures (Bozier et al., 2009; Lee, 1984b; Lindstedt and Michels, 1989). A typical presentation of

Shchelkin spiral can be found in Fig. 11, which was employed in Lindstedt et al.'s study on the investigation of deflagration to detonation transition of various alkane and alkene – air mixtures (Lindstedt and Michels, 1989).

The constructions of Shchelkin spirals have tremendous impact on the resulting explosion characteristics. The parameters to consider for the construction of these spirals include length, pitch and blockage ratio (BR). The various Shchelkin spirals, employed in Lindstedt et al.'s experiment and extracted in this review for discussion are presented in Table 2.

Fig. 12 is extracted from (Lindstedt and Michels, 1989), where Lindstedt et al. demonstrated that a minimum threshold flame speed at the obstacle exit is important in sustaining deflagration. They have concluded that a critical flame speed of ~250 m s^{-1} is required to achieve a quasi-stable propagation mode. This outcome emphasises that a quasi-stable strong deflagration regime most likely leads to transition from deflagration to detonation regime with adequate time and distance.

The pitch and blockage ratio for obstacles S/2 to S/7, presented in Table 2, are very similar. Keeping these parameters the same, the minimum lengths sustaining deflagration was 1.0 m for methane and 0.5 m for ethane as reported by the authors. Lindstedt et al. increased the obstacle lengths from 0.5 to 1.5 m (obstacles S/2 to S/7) for ethane–air mixture and found that the transition time from low speed flame to high speed flame reduces as the obstacle length increases. A reduction of 50% time was achieved when the obstacle length was increased from 0.50 to 1.25 m. While Figs. 12 and 13 were generated employing ethane–air mixture, they provide interpretations for other fuel–air mixtures including methane–air mixtures.

While methane is a weakly reactive fuel, the durations for the transition from deflagration to detonation in methane–air and ethane–air were found to be very close in the investigation of Lindstedt et al. Although the transition time for methane–air was slightly higher than that of ethane–air (28 vs 20.7 ms, obstacle S/5), the outcome of this investigation highlights the role of the obstacle-induced flame acceleration. The flame acceleration profile for methane–air mixtures employing obstacle S/5 is presented in Fig. 14. This figure illustrates the role of an obstacle in converting a low speed flame to a destructive explosion.

While obstacles accelerate flame propagation and transform the

Table 2
Description of various obstacles employed in Lindstedt et al.'s experiment and presented in this article.

Notation	Length (m)	Pitch	BR	Section (of total)
S/1	0.250	0.045	0.44	1 (1)
S/2	0.500	0.045	0.44	1 (1)
S/3	0.625	0.045	0.44	1 (1)
S/4	0.750	0.045	0.44	1 (1)
S/5	1.000	0.045	0.44	1 (1)
S/6	1.250	0.045	0.44	1 (1)
S/7	1.500	0.045	0.44	1 (1)
S/8	1.000	0.035	0.44	1 (2)
S/8	1.000	0.045	0.44	1 (2)
S/9	1.000	0.035	0.44	1 (3)
S/9	1.000	0.045	0.44	1 (3)
S/9	1.500	0.075	0.44	1 (3)

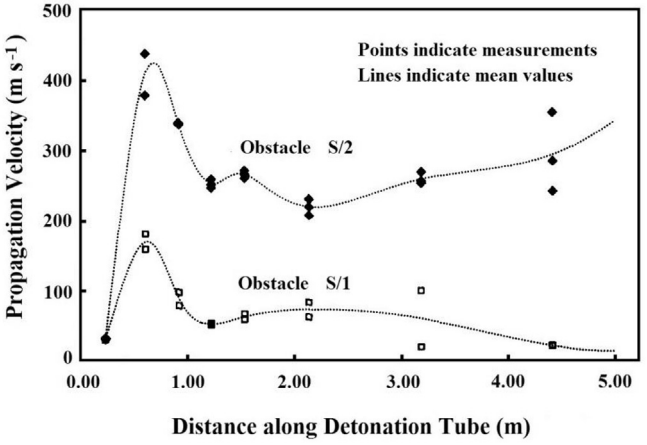

Fig. 12. Effect of short Shchelkin spirals on flame velocities along the tube in the explosion study of ethane–air mixtures of near stoichiometric ratios (Lindstedt and Michels, 1989).

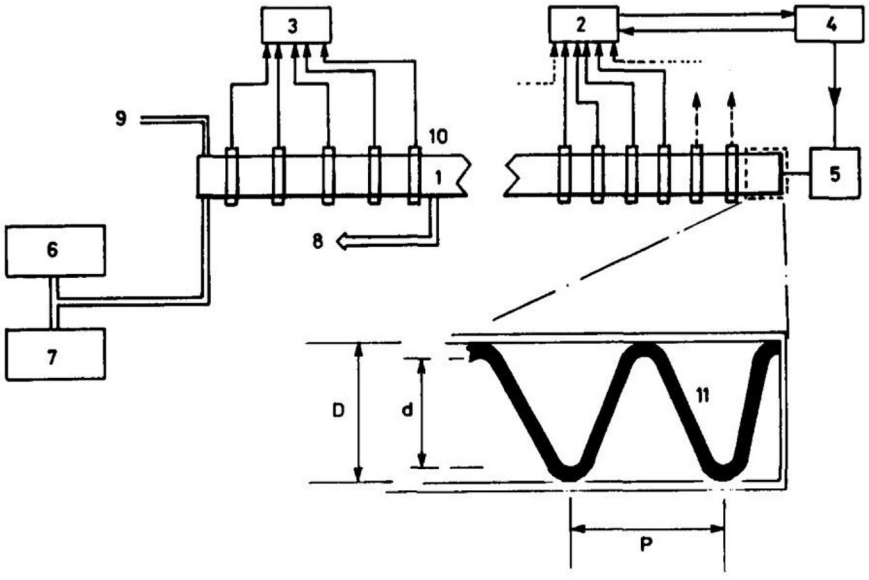

Fig. 11. Layout of Lindstedt et al.'s experimental setup: 1, detonation tube; 2, counter system 1; 3, counter system 2; 4, microcomputer with screening; 5, ignition source; 6, partial pressure mixing system; 7, flow mixing system; 8, mercury manometer; 9, to exhaust pump; 10, ionisation prove with amplifier; 11, Shchelkin spiral (Lindstedt and Michels, 1989).

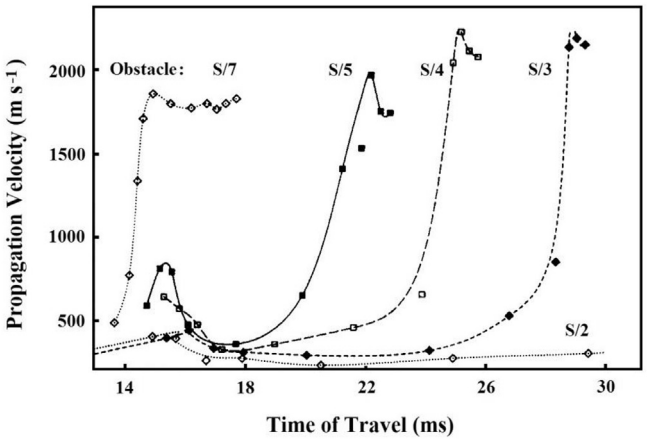

Fig. 13. The influence of the lengths of Shchelkin spirals on the time and the distance to the transition from deflagration to detonation or quasi-detonation (Lindstedt and Michels, 1989).

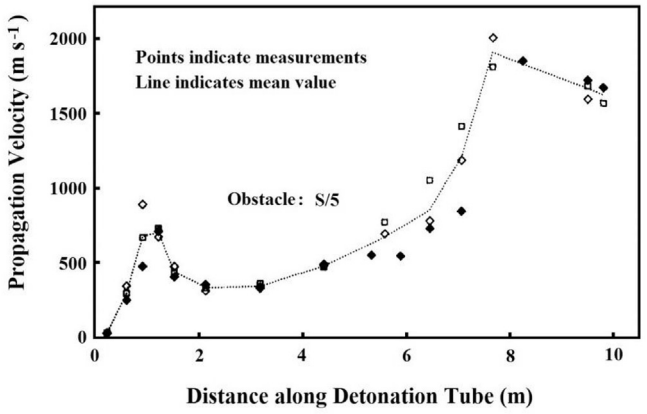

Fig. 14. Effect of 1 m long Shchelkin spiral with a pitch of 0.045 and a blockage ratio of 0.44 on the transition from deflagration to detonation or quasi-detonation for methane–air mixtures of near stoichiometry (Lindstedt and Michels, 1989).

flame to a more violent combustion wave, there is a maximum length of each design of obstacle above which flame speed reaches

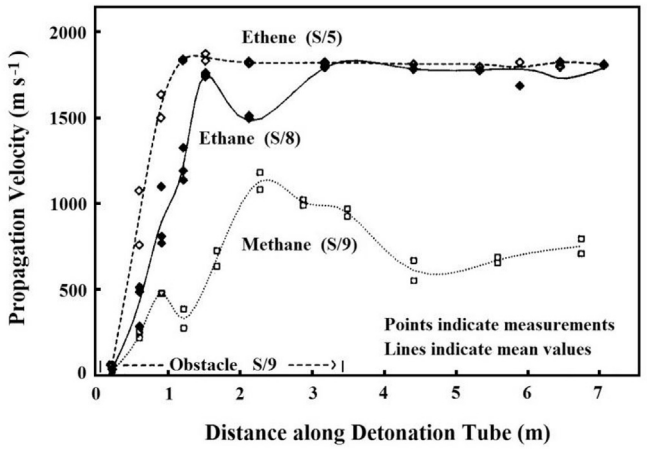

Fig. 15. Effect of longer Shchelkin spiral on the transition from deflagration to detonation or quasi-detonation for methane–air mixtures of near stoichiometry (Lindstedt and Michels, 1989).

a maximum value. As presented in Fig. 15 (Lindstedt and Michels, 1989), the increment of obstacle length from S/5 to S/8 did not increase the final exit flame speed for ethane–air mixture. The increment of obstacle length did not promote (from Figure 14 to Figure 15) transforming the quasi-detonation flame to detonation for methane–air.

The quasi-detonation flame speed for methane–air mixture, obtained in (Lindstedt and Michels, 1989), was close to speed at Chapman-Jouguet condition ($U_{obs}/U_{cj} = 0.79$ inside the obstacles and $U_{obs}/U_{cj} = 0.89$ in the smooth tube). Another study conducted by Lee with methane–air mixture employing Shchelkin spirals revealed a maximum flame speed of 800 m s^{-1} (Lee, 1984b). In contrast, the highest flame speed obtained by Lindstedt et al. was 1410 m s^{-1} for an obstacle with S/8 configuration. Nonetheless, this obstacle was effective in transforming deflagration to quasi-detonation for methane–air mixture.

5.2. Orifice plates

Orifice plates were found to be very effective in blocking the flow path and therefore generating turbulence. The parameter important for orifice plates is its blockage ratio (BR) and calculated from the relationship of $BR = 1\text{-}(d/D)^2$, where d is the orifice plate bore diameter and D is the inner diameter of the experimental duct (Lee et al., 1984). A number of researchers employed orifice plates to investigate flame acceleration from methane–air mixtures (Kessler et al., 2010; Kuznetsov et al., 2002; Lee et al., 1985, 1984; Peraldi et al., 1986). Kuznetsov et al., for example, employed orifice plates with BRs of 0.3 and 0.6 with the aim of investigating transition of deflagrating flame to detonation from methane–air mixtures of a range of methane concentrations. In order to test the effect of orifice plates, they employed two types of experimental setups. One of them was constructed with a 12 m long tube with an inner diameter of 174 mm, while the other setup was comprised of a 34.5 m long tube with an inner diameter of 520 mm.

Fig. 16 illustrates the outcome of Kuznetsov et al. from experimental setups operating with orifice plates of 174 and 520 mm diameter with a same BR of 0.3. Quasi-detonation regimes were observed for 9.5, 10.5 and 12% methane when experimental setup of 520 mm orifice plate was employed. For experimental setup of 174 mm orifice plate, the quasi-detonation regime was limited to 9.5 and 11% methane mixtures.

Flame acceleration reduces with increased blockage ratio of orifice plate. Peraldi et al. reported that quasi-detonation regime was not achieved when examining flame acceleration, employing orifice plates of 0.43 blockage ratio in a 18 m long tube with an inner diameter of 300 mm (Peraldi et al., 1986). Similar phenomenon was observed in the studies of Kuznetsov et al. (Fig. 17) for both of their experimental setups (as described previously) with orifice plates of 0.6 blockage ratio. The maximum velocities achieved with 0.6 BR orifice plates were much lower than the quasi-detonation flame velocities.

One important parameter in measuring detonation sensitivity or detonability is detonation cell size or width, λ (Gavrikov et al., 1999). There are several methods to determine detonation cell width. Historically (in sixties (Guirao et al., 1989)) and in recent researches (Kuznetsov et al., 2002), smoked foil techniques were used to determine the detonation cell width. The second method of estimating this parameter is to analyse the structure of the pressure signal behind the detonation wave, known as pressure oscillation technique as demonstrated by Dorofeev et al. (Dorofeev et al., 1992). In addition, Gavrikov et al. developed a theoretical model, often called as Gavrikov model, which can predict detonation cell width (Gavrikov et al., 2000).

When the diameter of orifice plate is divided by detonation cell

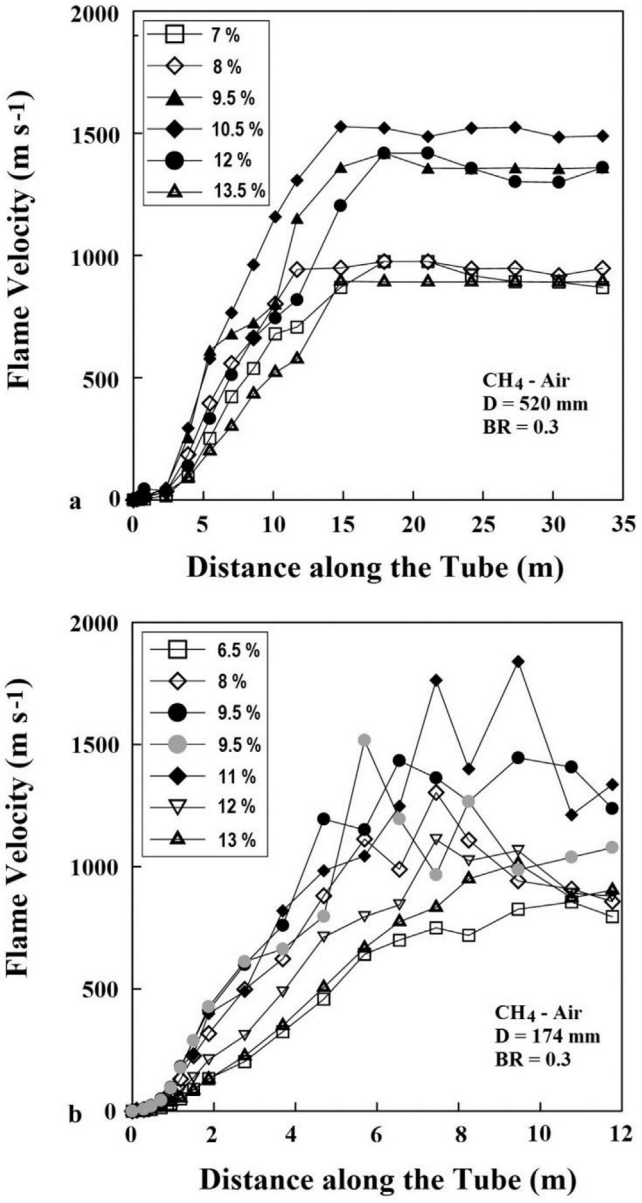

Fig. 16. Effect of orifice plates with 0.3 blockage ratio on flame speed in tubes of two different diameters (520 and 174-mm) (Kuznetsov et al., 2002).

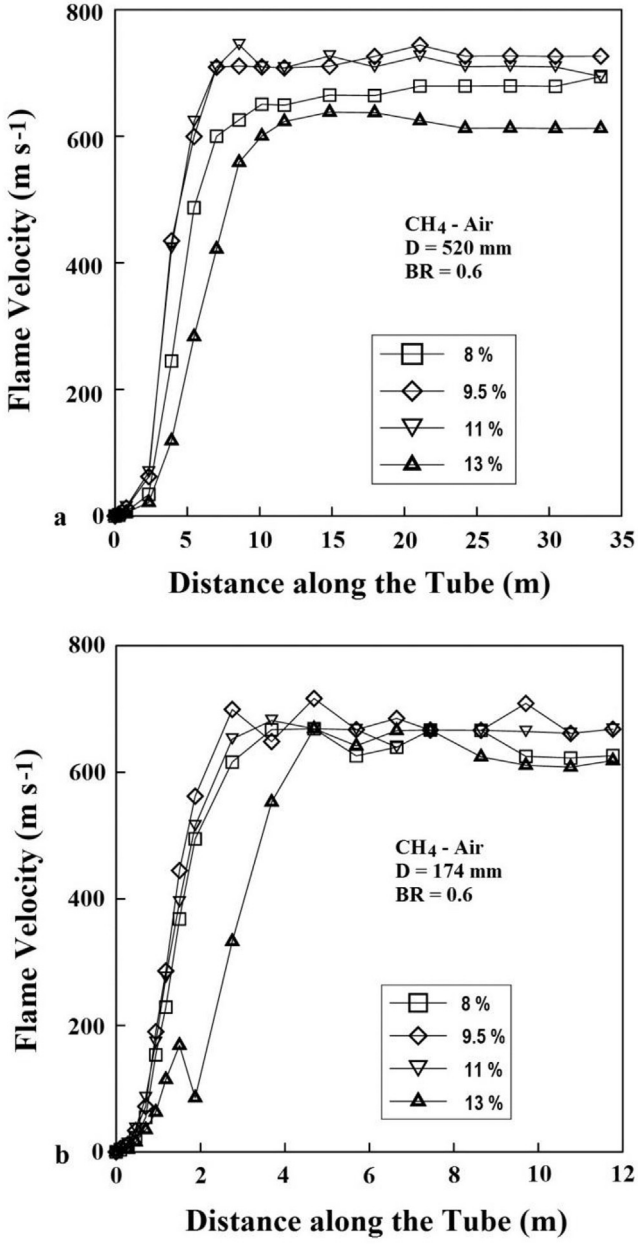

Fig. 17. Effect of orifice plates of 0.6 blockage ratio on flame speed in tubes of two different diameters (520 and 174-mm) (Kuznetsov et al., 2002).

width, the obtained ratio (d/λ) provides some interpretation in terms of finding possibilities of transition from deflagration to detonation. Researchers found that the ratio of d/λ needs to be greater or equal to 1 in order to obtain detonation. Fig. 18, extracted from the investigations of Kuznetsov et al., replicated the findings of other researchers (Dorofeev et al., 2000; Peraldi et al., 1986). While DDT was observed for a d/λ value slightly higher than 1 for orifice plates of 0.3 BR, no DDT was found for orifice plates of 0.6 BR for d/λ value up to 1.8. This means that the higher the blockage ratio, the higher the required d/λ value to reach DDT.

Dorofeev et al. showed an additional criterion, similar to $d/\lambda \geq 1$, to characterise DDT (Dorofeev et al., 1994, 1996, 2000). They found that the ratio of L/λ, where L was defined as a characteristic size of a room filled with combustible mixture (for obstructed channels, L is the length of the channel), could be used as a criterion for DDT. The length of the obstructed channel can be mathematically defined as $L = (S + D)/2/(1-d/D)$, where S is the obstacle spacing and D is the inner diameter of the experimental tube. When $S = D$, DDT may be observed for $L/\lambda \geq 7$. As illustrated in Fig. 19, DDT was found for a L/λ value slightly higher than 7 for 0.3 BR plates. However, no DDT was observed for 0.6 BR orifice plates meaning that the L/λ value for these plates needed to be higher to obtain DDT.

To conclude, the outcomes of orifice plate investigations by various researches similarly determine that a narrower channel in explosion scenarios can accelerate a low speed flame to violent explosions.

5.3. Obstacles of various shapes

Various shaped obstacles, such as square, triangular and circular, were found to accelerate flame propagation in a number of studies (Chan et al., 1983; Ciccarelli et al., 2010; Gamezo et al., 2008;

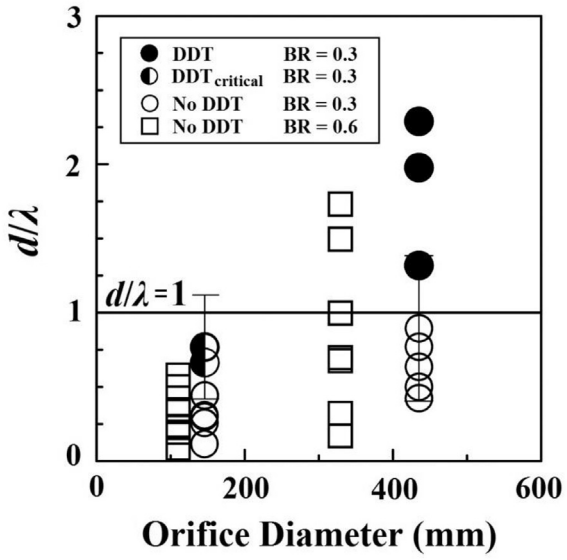

Fig. 18. The relationship of d/λ ratio and DDT in the explosion study (Kuznetsov et al., 2002).

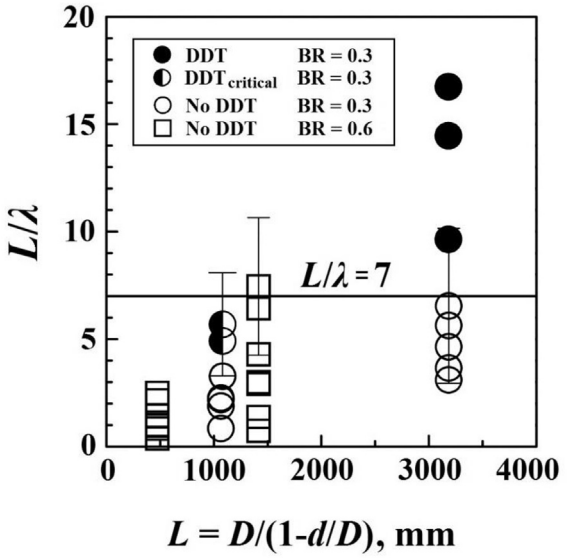

Fig. 19. The relationship of L/λ ratio and DDT in the explosion study (Kuznetsov et al., 2002).

Johansen and Ciccarelli, 2009; Kessler et al., 2010; Kindracki et al., 2007; Li et al., 2015; Moen et al., 1982; Park et al., 2007; Phylaktou and Andrews, 1991; Yi et al., 2011; Zhiming, 2010). Similar to orifice plates, blockage ratio due to the placement of these obstacles is an important parameter in explosion studies. For these obstacles, blockage ratios are normally estimated by the term, BR = A_o/A_d, where A_o is the largest cross-sectional area blocked by the obstacle and A_d is the inner cross-sectional area of the explosion duct (Ibrahim and Masri, 2001; Park et al., 2007). Johansen et al., for instance, employed an array of rectangular obstacles mounted at the top and bottom surfaces in modular both end closed combustion channels constructed from four modules (Johansen and Ciccarelli, 2009). They used obstacles with three blockage ratios of 0.33, 0.50 and 0.67. When conducting experiments with methane–air mixture at stoichiometric ratio, they found that the flame acceleration increased with the increment of blockage up to approximately one-third of the combustion channel width. For the remaining two-thirds of the combustion channel, the flame acceleration became the highest with obstacles of 0.50 blockage ratio. This means that there is an optimum value of blockage ratios for which the flame acceleration reaches a maximum for the majority of the combustion channels.

Zhiming et al. reported the effect of the number of obstacles in the flow path, studied numerically for methane–air mixtures of stoichiometric conditions (Zhiming, 2010). In their simulation, a two-dimensional model for a one end open and one end closed pipeline was considered. It was found that the overpressure of the shock wave front increased with increasing number of obstacles. Similar phenomenon was observed for flame speed (Fig. 20). The peak flame speed increased with an incremental increase in the number of obstacles in the flow path. In addition, the number of peak values for flame velocities increased with the incremental increase in the number of the obstacles.

Park et al. employed cylindrical, triangular and square bars in an explosion chamber with ventilation area at the top surface while conducting explosion studies with methane–air mixtures with a methane concentration of 10% (Park et al., 2007). They positioned their obstacles in a way that their blockage area may be described as $A_o = lx$, where l is the length of the bar and x is the diameter of the circular area for the cylindrical bar or a side for triangular or square bar. For the same blockage ratio, pressure rise was highest with the cylindrical bar while it was lowest with the square bar. In contrast to the findings of Park et al., Ibrahim et al. (Ibrahim and Masri, 2001) observed the lowest pressure rise with cylindrical bars and the highest with the wall/plate type obstacles while conducting explosion study with liquefied petroleum gas (LPG) of 88% C_3H_8, 10% C_3H_6 and 2% C_4H_{10} employing an explosion chamber. Park et al. described that the configuration of the explosion chamber affected in the resulted pressure rise. In comparison to the study by Ibrahim et al., Park et al. employed an explosion chamber with low L/D ratio, large vent area and a smaller distance between the ignition point and the chamber exit. The confinement in the investigation by Park et al. was much lower than the experiments conducted by Ibrahim et al. The huge difference in confinement resulted in a reverse trend in pressure rise in Park et al.'s experiments.

In summary, the blockage ratio has tremendous effect on the flame acceleration. It was found in an experimental investigation that the value of flame acceleration primarily increases with blockage ratio for a certain length in a combustion channel. For the remainder length of the channel, the value of flame acceleration reaches a maximum value for a particular blockage ratio. As discussed above, the repetition of obstacles enhances the effect of obstruction. In addition, the shape of the obstacles and the geometry of the explosion gallery affect the pressure in an explosion. Mechanistically, when obstacles are placed in the flow path of a burning gas, vortices are formed. As the flame propagates, small-sized vortices convert to large-sized vortices. This accelerates the reaction rate of the combustible materials and therefore, both the peak pressure and flame speed increase.

Confinement or lack of ventilation is always a concern in coal mines. The confinement varies from one coal mine to another. In conjunction with the physical structure of a coal mine, machines and additional mining infrastructure add confinement to the coal mine. The investigations with various obstacles provide an understanding of the impacts of confinement on flame acceleration. As the degree of confinement increases, the velocity at which flame propagates in mines increases.

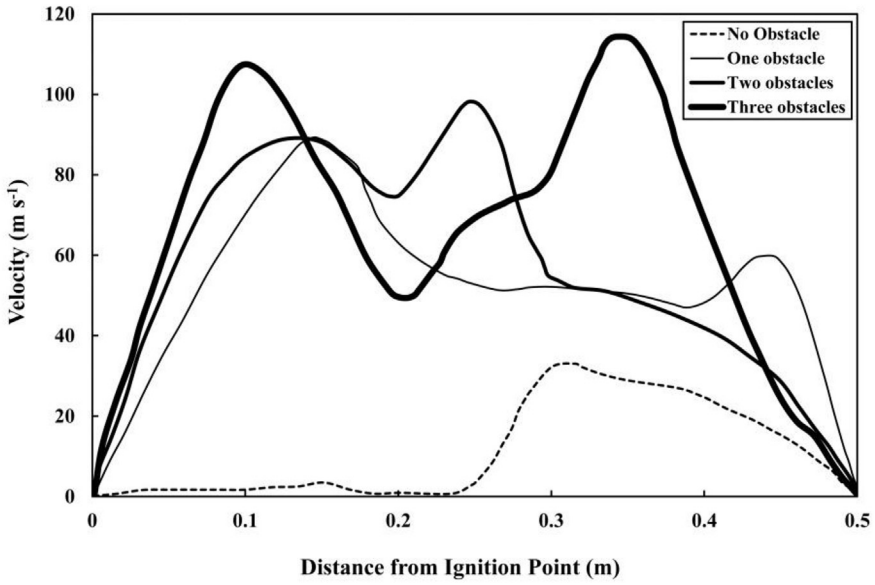

Fig. 20. Effect of rectangular obstacle/s on flame speed in the explosion study of methane–air mixtures (Zhiming, 2010).

5.4. Wall roughness

The wall roughness of an experimental tube is an important parameter in explosion studies. This parameter needs to be accounted for when collecting data employing rough tubes. Higher wall roughness reduces the time (Liberman, 2008) and also distance (Baker et al., 2012) of the transition from deflagration to detonation. This is mostly because the detonation wave experiences turbulisation due to the inhomogeneities present in rough tubes (Zel'dovich et al., 1987). However, it was observed that the detonation velocity reduces in rough tubes. This is because strong friction is present in rough tubes leading to momentum loss of the flow (Gelfand et al., 1993).

Gelfand et al. conducted a theoretical study in understanding explosion characteristics in molten tin and water. They reported the detonation wave velocity as a function of C_f/R (Fig. 21, C_f is the wall drag coefficient and R is the tube radius). The tube roughness and its diameter are related when estimating detonation velocity. This means that tubes with lower diameter will require smaller wall roughness to produce a similar effect on detonation velocity compared to tubes of larger diameter. In any case, Fig. 21 represents

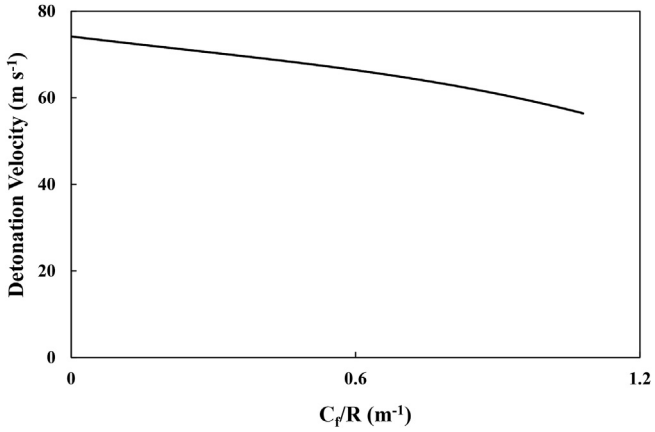

Fig. 21. Effect of tube roughness on detonation velocity in the explosion study of molten tin-water system (Gelfand et al., 1993).

that the detonation velocity reduces with increasing tube roughness for tubes of certain diameters. Similar findings were found in the theoretical study of Zel'dovich et al. (Zel'dovich et al., 1987) where they considered several fuels including methane. While Zel'dovich et al. showed that the presence of friction reduces the detonation velocity, they also found that the reduction of detonation velocity is dependent on the activation energy of the fuel.

In short, the wall roughness of tubes reduces the transition time and distance for the transformation of deflagrated flame to detonation. However, the momentum loss due to the friction of the tube roughness results in reduction of peak pressure and therefore, the flame becomes less violent compared to the flame progress in smooth tubes.

The knowledge of tube roughness on the transformation of deflagrated flame to detonation can be applied in coal mines. In many places, the passages of coal mines are constituted by rough surfaces. Increased roughness of surfaces in mine passages will result in quicker transition of deflagrated flame to detonation. In addition, this transition will occur in a shorter distance as explained previously.

6. Explosion characteristics in vessels and smooth tubes

The degree of confinement immensely impacts on flame acceleration. The pressure rise is expected to be higher with increasing degree of confinement. Confinement may be introduced by obstacles, as described in sections 5 and 6, or by geometry of the explosion chamber. For example, a closed vessel may be defined as a confined system while an open ended smooth tube may be termed as a semi-confined system. The degree of confinement (ϕ) of a vessel may be defined as (Chan et al., 1983):

$$\phi = 1 - \frac{\textit{open area on permeable wall per unit length of the vessel}}{\textit{total surface area per unit length of the vessel}}$$

This equation provides an understanding on confinement. When there is no opening on side walls, the vessel is fully confined. Similarly, for smooth tubes, when one end is closed, the system becomes confined. The introduction of obstacles such as orifice

plates and Shchelkin spirals increases the degree of confinement in smooth tubes.

Methane–air or methane–oxygen–nitrogen mixtures of large volume were employed in previous researches in unconfined systems (Bull et al., 1976; Nicholls et al., 1979; Parnarouskis et al., 1980). While there are restrictions for flame propagation in smooth tubes and vessels, the explosion develops in all three spatial dimensions in these unconfined systems (Zipf et al., 2013). Those researches revealed that it is very unlikely to reach sustainable detonation pressure waves from methane–air mixtures in unconfined systems. For a particular volume of combustible-air mixture and at the self-sustaining point of its combustion $E_g > E_l$, where E_g is the generation of thermal energy due to combustion of the flammable gas and E_l is the loss of energy due to the sharp rise of local temperature to final flame temperature (Carroll). In unconfined systems, the energy loss (E_l) is usually very high and therefore, E_g becomes equal to E_l and the condition of $E_g > E_l$ is not reached. Therefore, the combustion pressure wave is not sustained.

Several researchers employed vessels and smooth tubes with the aim of understanding explosion characteristics of methane–air systems. The outcomes of these researches reveal pressure characteristics, determine velocity profile (often presented as Mach number profile) and estimate detonation cell width or size. The outcomes are largely depended on the geometries of the investigated explosion chamber or, in other words, on confinement. Zhang et al., for instance, employed a 10 m^3 closed vessel of 2.0 m diameter, 3.18 m length and a wall-thickness of 0.045 m and their study relates to explosion in confined space (Zhang et al., 2014). Explosion pressure data were collected at 0.25, 0.50, 0.75, 1.30 and 1.80 m from one end of the vessel employing pressure gauges. The maximum explosion pressure was found for 9.5% methane concentration in air (Fig. 22). This outcome is consistent with the understanding as described in section 2.

With the aim of predicting explosion characteristic from methane–air mixtures, an experimental setup constituted of 30 m long and an inner diameter of 0.456 m with one end closed (semi-confined) duct was constructed employing schedule 80 mild steel pipes at the University of Newcastle, Australia. The initial experimental setup was employed to collect data on explosion parameters, particularly explosion pressure, with the intention of applying them in the implementation of explosion mitigation measures in coal mines.

The experimental setup (Fig. 23) was a modular design and consisted of 11 cylindrical modules, attached together with flanges. Each module had three pressure transducers located radially at 120° at the centre of the each module length. The first section, termed as the ignition section, is module B1 where 9% methane was employed for ignition. This section was isolated from the proceeding section, termed as secondary explosion section, by a temporary inflated balloon. The secondary explosion section is comprised of one or more modules. Similar to module B1, module A2 was comprised of one balloon port and methane injection system. This secondary explosion section was constructed by positioning A2 module after B1 module and the section size could be adjusted by moving the module A2 to different locations along the length of the tube (e.g., A3, A4 etc.) as can be seen in Fig. 23.

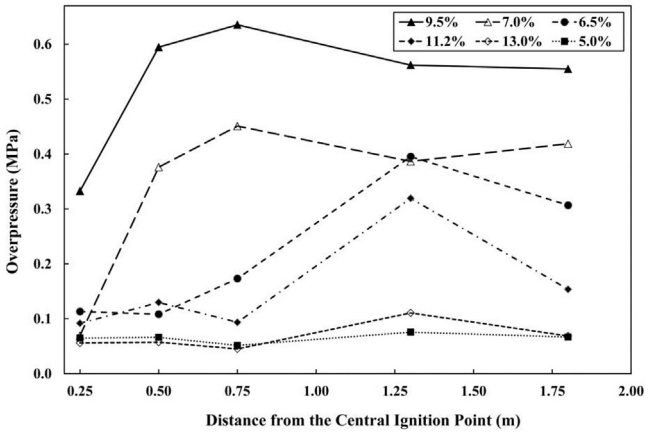

Fig. 22. Explosion overpressures measured in a closed vessel in the explosion study of methane–air mixtures (Zhang et al., 2014).

Fig. 24 was constructed from data maintaining the length of secondary explosion section only with the module A2. Average peak pressures of three sensors were plotted in Fig. 24. Therefore, the ignition section was of 2 m while the secondary explosion section was of 3 m. In this scenario, the pressure profile is quite different compared to Fig. 22. While the pressure initially increased and then decreased in Fig. 22, the pressure gradually dropped in Fig. 24. The pressure drop was caused by the one end open geometry of the experimental setup employed for Fig. 24 compared to the closed vessel employed for Fig. 22.

Similar geometry of 73 m long one end closed tube with a diameter of 1.05 m was employed by Zipf and co-authors (Zipf et al., 2013). In their experiments, fresh air was ensured inside the explosion tube by running a portable fan for 30 min (Gamezo et al., 2012). The open end was then closed by a thin plastic diaphragm (0.15 mm thick) and methane was then introduced into the system by a blower fan and circulated to ensure proper mixing. This process assisted them to obtain homogeneous methane–air mixtures inside the explosion tube with predetermined equivalence ratios.

To initiate ignition, a non-electric blasting cap was employed at approximately 0.5 m from the closed end inside an igniter bag. The igniter bags, constructed by 0.15 mm thick plastic, were of cylindrical shapes and had a diameter of 1 m. The bags were filled with a stoichiometric methane–oxygen mixture and placed at the closed end of the tube. In most cases, the igniter bag volumes were 2.9 m^3, however, in some experiments 3.25 m^3 igniter bags were employed.

Fig. 25 represents a test conducted by Zipf et al. while studying direct initiation detonation employing methane–air mixtures. This figure was constructed when they used 10% methane in air mixture with an igniter bag volume of 2.9 m^3. According to their theoretical calculation by the software CHEETAH, the Chapman-Jouguet detonation pressure for this combination is 1.758 MPa and the detonation velocity is 1828 m s^{-1}. Their experimental investigations resulted in a detonation pressure of 1.5 MPa and a detonation velocity of 1831 m s^{-1}. While the experimental and theoretical detonation velocities were very similar, the detonation pressure was 14.7% lower in the experimental results as compared to theoretical calculation. At these conditions and configuration, the shock pressure wave and flame propagate at similar speed. As can be seen in Fig. 25 where both of them almost superimpose along the tube.

As described previously, Zipf et al. employed 3.25 m^3 igniter bags in a separate set of experiments. The velocity profile (Fig. 26) and the pressure profile (Fig. 27) were generated including data from both sets of experiments (2.9 and 3.25 m^3 igniter bags). There were a few data points far away from the expected trend. According to their explanation, these data points resulted from premature failure of the plastic bags they employed for their investigations. The maximum pressure and velocity was found at 10% methane in air, which is slightly higher than the stoichiometric mixture of methane–air. The maximum pressure and maximum velocity obtained in the experiments were close to theoretical Chapman-Jouguet values (calculated by the software CHEETAH and

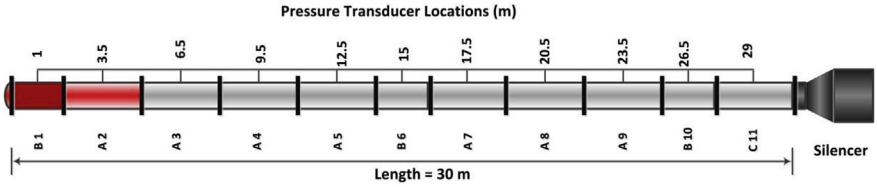

Fig. 23. Schematic diagram of detonator tube employed at the University of Newcastle, Australia.

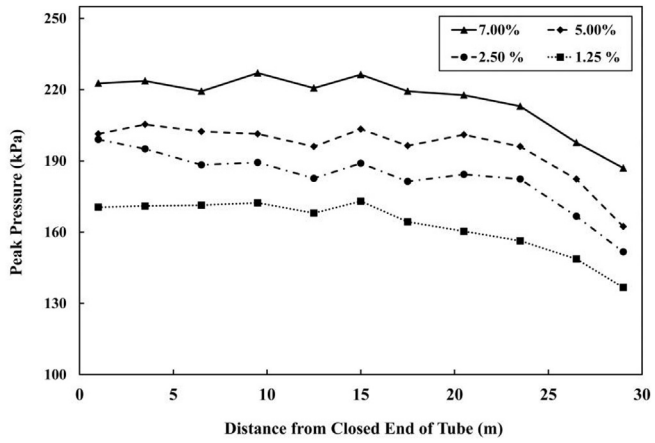

Fig. 24. Pressure profile obtained from the explosion study of methane–air mixtures at the University of Newcastle, Australia.

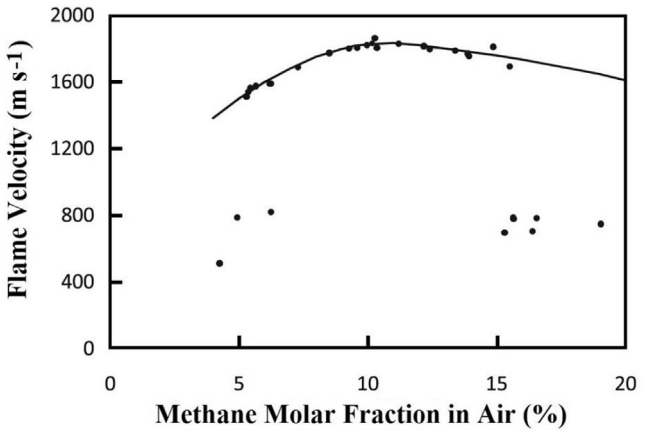

Fig. 26. Experimental (data points) and theoretical (solid line) detonation velocities obtained from the investigations of Zipf and co-authors for methane–air explosive mixtures (Zipf et al., 2013).

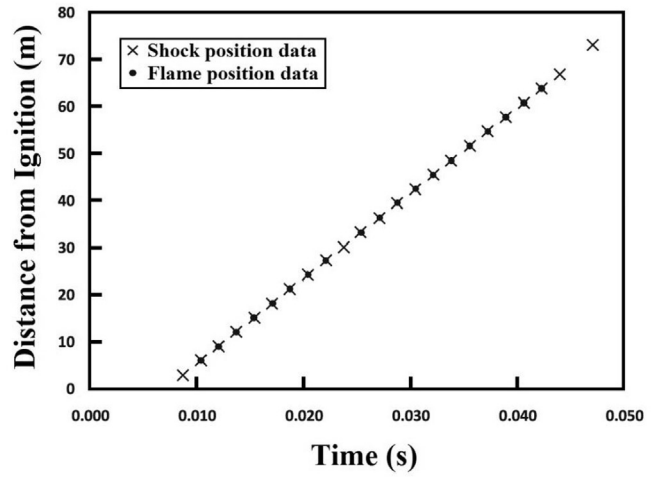

Fig. 25. Shock and flame positions with respect to time as obtained from the investigations of Zipf and co-authors for an explosive gas mixture of 10.0% methane in air (Zipf et al., 2013).

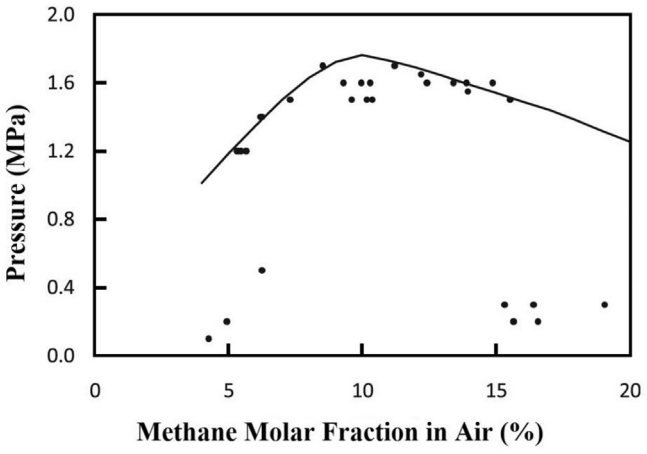

Fig. 27. Experimental (data points) and theoretical (solid line) detonation pressure values obtained from the investigations of Zipf and co-authors for methane–air explosive mixtures (Zipf et al., 2013).

presented as solid lines in Figs. 26 and 27).

Zipf et al. employed smokefoil tests to determine the detonation cell sizes using methane concentrations of 5.3–15.5% in air (Fig. 28). When compared to experiments carried out with various methane–air mixtures, the detonation cell size was found to be the lowest (~25 cm) for the experiment conducted with methane–air mixture of near stoichiometric condition (10.2% methane in air). However, the number of detonation cells was highest (8) at that condition (10.2% methane in air). In contrast, the detonation cell sizes were 55 and 61 cm for methane concentrations of 7.3 and 14% in air while the cell numbers were 3 and 4 respectively for those concentrations.

Briefly, the confinement is very important in terms of the severity of explosion. The higher the confinement is, the higher the explosion pressure. However, according to the tests conducted by researchers, semi-confinement is also enough to obtain detonation or quasi-detonation.

The pressure and flame velocity profiles of explosions obtained in various researches are helpful in simulating actual coal mine explosion scenarios. The geometries of coal mines are diverse in nature and therefore, the outcomes of various shapes of experimental setup are important in understanding the nature of explosion in coal mines. The results of various investigations thus provide a picture of coal mine explosions and assist in designing

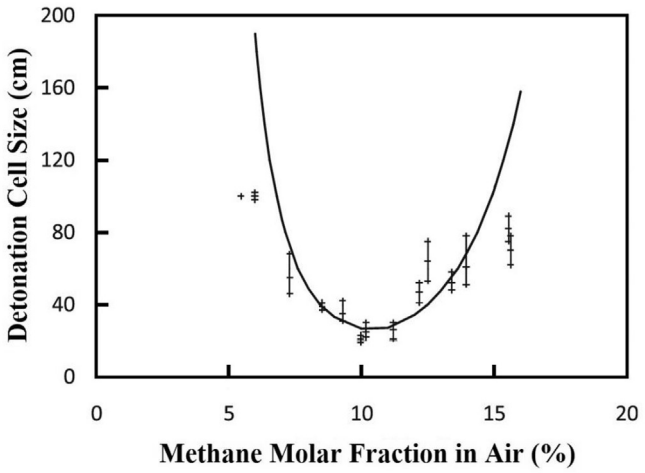

Fig. 28. Experimentally measured detonation cell size (low, high, and average data points) and cell size model (solid line, calculated by the model developed by Gavrikov et al. (Gavrikov et al., 2000)) as found in the investigations of Zipf for methane–air explosive mixtures (Zipf et al., 2013).

explosion mitigation systems.

7. Impact of tube diameter on attaining DDT in methane–air mixtures

Researchers conducted investigations on methane–air explosions employing experimental setups of various tube diameters (Kogarko, 1958; Matsui, 2002; Oran et al., 2015; Wolański et al., 1981). Oran et al. constructed a figure which provides general information on the size of explosion tubes required to achieve detonation for methane–air mixtures (Fig. 29) (Gamezo et al., 2012; Oran et al., 2015; Zipf et al., 2014). Fig. 29 suggests that a wide range of tube diameters can be employed to achieve detonation from methane–air mixtures of stoichiometric condition. However, deviations from stoichiometric condition reduce the range of tube diameters at which detonation is possible from the methane–air mixture.

The area under the curve in Fig. 29 may be explained as the detonation limit of explosion tubes for methane–air mixtures (Gamezo et al., 2012). The limit is narrow for explosion tubes of smaller diameter and widens with increasing tube diameter. In large tubes, the energy released accelerates fast enough to cause shock compression and therefore, a wider range of methane–air mixtures can develop supersonic flames (Gamezo et al., 2012).

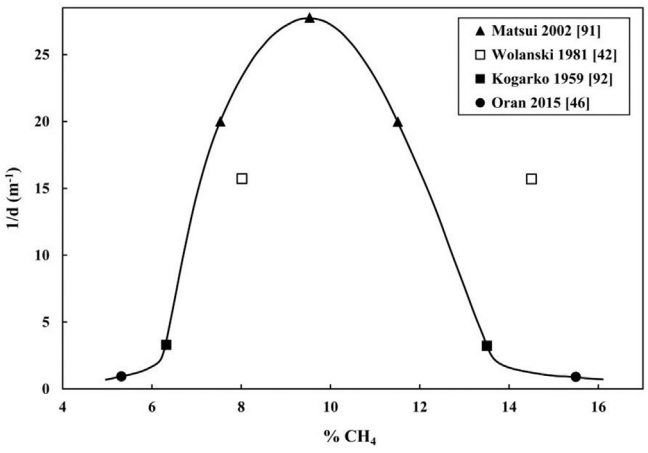

Fig. 29. Effect of tube diameter achieving DDT for methane–air explosive mixtures (Oran et al., 2015).

Consideration of tube diameter is important for installation of any duct in coal mines. Several types of ducts, such as ventilation duct and explosion vent duct, are installed in coal mines. As can be seen in Fig. 29, larger diameters of ducts favour DDT. Therefore, proper consideration of duct diameter is required in the design of any duct for coal mines to reduce the chance of DDT.

8. Effect of geometric scale on explosion characteristics

An actual mine gallery is several hundred times larger than the experimental ducts employed by various researchers. A question therefore remains on the scalability of the data obtained from those experimental investigations. With the aim of understanding the effect of geometric scale on various explosion parameters such as peak pressure and flame speed, Zhang et al. conducted a study on methane–air mixture for a methane concentration of 10% (Zhang et al., 2011a,b). They employed a commercial software package, known as AutoReaGas, to understand the explosion parameters. The software is comprised of two solvers – a gas explosion solver and a blast solver, where the solvers are based on Navier-Stokes and Euler equations respectively. The software was previously verified in studying gas explosion behaviour with obstructed channels (Salzano et al., 2002).

Three geometric scales, 1:1, 1:10 and 1:100 were chosen for the calculations. The details of the scales are presented in Table 3. For instance, in the case of the 1:1 scale or full scale, a 500 m straight mine gallery with a square cross-section of 2.45 m × 2.45 m was considered. The first 100 m of the mine gallery was assumed to be filled with methane–air mixture. In order to add obstacles in their calculations, they considered steel support bars of 100 mm × 100 mm dimensions positioned at 1 m intervals in the longitudinal direction of the mine gallery. One end of the mine gallery was considered to be closed while the other end was assumed to be open. Similar description applies to 1:10 and 1:100 scales.

The study of Zhang et al. revealed that the flame becomes catastrophic in larger scales. Zhang et al. plotted the pressure data against scaled distance (Fig. 30) (Zhang et al., 2011a). The dimensionless parameter, scaled distance (L/φ, where L is the distance from the ignition point to a certain point of the mine gallery and φ is the width or height of a cross-section of the gallery) was used to plot and compare data of all scales. At a scaled distance of 40.82, the overpressure for the full scale was found to be 1.260 MPa while the overpressure dropped to 0.9991 and 0.8280 MPa for the smaller scales of 1:10 and 1:100 respectively (Zhang et al., 2011b).

The flame speed was also found to be higher for full scale calculations. As presented in Table 4, the flame speed was obtained to be 733.44 m s^{-1} for full scale while it dropped to 550.00 m s^{-1} for a one hundredth size theoretical mine gallery. As discussed previously, experimental explosion studies are carried out in much smaller scale compared to actual coal mines. According to the above examination, the explosion pressure and flame velocity are expected to be higher in real coal mine situations compared to data in open literature from small scale apparatus. The geometric scale is therefore required to be factored in while applying experimental data in the simulation of actual coal mine explosions.

9. Criteria for attaining DDT in smooth tubes

A number of criteria are important when investigating detonation in smooth tubes. Zipf et al. summarised a few of them (Zipf et al., 2013). They addressed three criteria including the tube

Table 3
Details of geometric scales employed in the study of Zhang et al. (Zhang et al., 2011a,b).

Scale	Cross sectional area (m^2)	Length (m)	Methane–air mixture retention length (m)	Dimension of support bar (mm)	Intervals at which support bars were positioned (m)
1:1	2.45 m × 2.45 m = 6 m^2	500	0–100 m	100 mm × 100 mm	1 m
1:10	0.245 m × 0.245 m = 0.06 m^2	50	0–10 m	10 mm × 10 mm	0.1 m
1:100	0.0245 m × 0.0245 m = 0.0006 m^2	5	0–1 m	1 mm × 1 mm	0.01 m

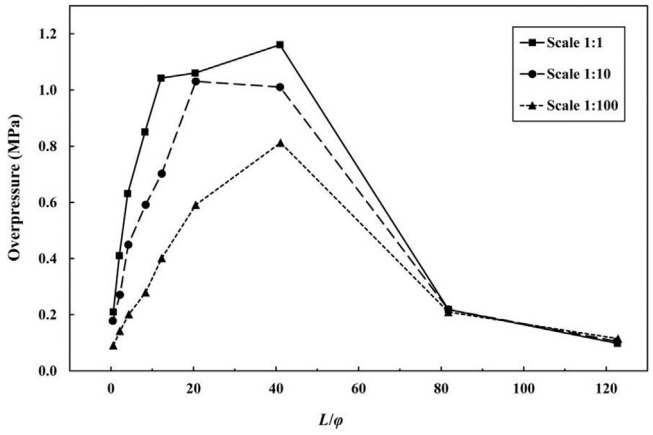

Fig. 30. Effect of geometric scale on pressure rise as obtained in the explosion study of methane–air mixtures (Zhang et al., 2011a).

Table 4
Average flame speed (m s^{-1}) in various geometric scales in the study of Zhang et al. (Zhang et al., 2011b).

Scaled distance	Scale 1:1	Scale 1:10	Scale 1:100
0–0.41	2.88	3.57	2.91
0.41–40.82	733.44	722.63	550.00
40.82–81.63	467.3	422.48	438.60

length, diameter and geometry. The diameter of the tube required to achieve DDT depends on detonation cell size. The relationship between the tube diameter and detonation cell size is $d/\lambda \geq 1$ as discussed in section 5.2. Employing the smokefoil test, Zipf et al. reported a detonation cell size of 25 cm for a near stoichiometric mixture of methane–air (10.2% methane in air) (Gamezo et al., 2012; Zipf et al., 2013). This means that the diameter of the tube needs to be higher than 25 cm if a stoichiometric methane–air mixture is employed. While conducting experiments outside of a stoichiometric methane–air mixture, Zipf et al. found larger values of detonation cell sizes. For a methane concentration of 7.3% the detonation cell size became 55 cm while the value of detonation cell size was 60 cm for the experiment conducted with a methane concentration of 14%.

The criterion for the length of the tube is also discussed in section 5.2, which is $L/\lambda \geq 7$. As methane–air mixtures are weakly reactive systems, a much larger value of L/λ is required to achieve detonation. There is another way of describing the required length of the tube to obtain detonation. Instead of referring L/λ ratio, L/D ratio is often presented in the literature. For instance, Zipf et al. employed a L/D ratio of slightly higher than 70. With this condition they achieved 14.7% less pressure than the Chapman-Jouguet pressure when a methane–air mixture slightly higher than the stoichiometric ratio was applied. This means that the L/D ratio needs to be higher than 70 in order to achieve detonation from a methane–air mixture. If we compute an explosion tube diameter equivalent to detonation cell size, then L/λ needs to be higher than 70 for methane–air mixtures of stoichiometric condition.

The tube geometry needs to be strong enough to handle the detonation pressure. In the wall of the experimental tube, the shock wave may reflect several times off the Chapman-Jouguet pressure (Landau and Lifshitz, 1987). Therefore, a safety factor needs to be included while designing explosion tests with smooth tubes. In constructing a 73 m long detonation tube with a diameter of 1.05 m, Zipf et al. employed a mild steel tube of 9.5 mm thickness with a minimum yield strength of 248 MPa and an ultimate tensile strength of 414 MPa. These values may be a guideline for understanding the geometry required to test detonation in a smooth tube.

Apart from the criteria related to explosion tube, the energy of ignition source and the mass of combustible material play important roles in the resultant explosion pressure. In general, higher ignition energies are favourable to obtain detonation pressure. If low ignition energy is applied, the reaction zone gradually isolates from the pressure wave and the final explosion becomes limited to deflagration (Lee, 1984a). Therefore, no transition occurs to obtain detonation.

The higher the mass of combustible material, the higher the chance of achieving detonation. The volume of explosion tube, Zipf et al. employed was 63.4 m^3 (Gamezo et al., 2012; Zipf et al., 2013). The volume of methane–air mixture (10.2% methane in air) resulted in quasi-detonation (pressure value was 14.7% lower than Chapman-Jouguet pressure value) when a 2.9 m^3 ignitor bag containing a stoichiometric methane–oxygen mixture was employed. The combination of the ignition energy from the igniter bag and the content of the combustible gas in the explosion tube (60.5 m^3) established a quasi-detonation in the experiment of Zipf et al. This relationship between of the ignition energy source and the volume of explosive gas is important to obtain DDT. If a lower amount of methane–air mixture is employed, a higher ignition energy will be required.

In summary, the mass of combustible material, the energy of ignition source and the length, diameter and geometry of explosion tube are important criteria in reaching DDT in a smooth tubes. For any coal mine passage, these criteria can provide predictions on the nature of explosions. In addition, any duct that may be installed for ventilation or explosion vent purposes needs to be designed including these considerations.

10. Summary

Various outcomes from the possibilities of initiation of explosions from methane–air mixtures have been discussed in this review. The impacts of the concentrations of methane–air mixtures and ignition energies have been examined. Studies revealed that a methane concentration of ~9.5% is the most dangerous mixture for methane–air systems. The lower flammability limit (LEL) of methane was found to be 4.6 ± 0.3% and the upper flammability limit (UEL) of methane was obtained 15.8 ± 0.4% from various investigations when methane was ignited in air at ambient temperature and pressure.

Ignition of a combustible gas may be initiated via auto-ignition

or by an external ignition source such as an electric spark or flame. The reported auto-ignition temperature for methane in air starts from 537 °C.

Combustible gas-oxygen mixtures were often employed to initiate ignition. The total chemical energy of the gas mixture was found to affect the final explosion. It was found that a high level of ignition energy is favourable in obtaining a devastating detonation.

When conducting explosion studies in cylindrical tubes, the diameters of the tubes were found to be important in obtaining DDT. A wide range of methane–air mixtures can lead DDT for larger diameter tubes. The range of methane–air mixture that can produce DDT is narrow for small diameter tubes.

The explosion studies were conducted mostly with small size setups. However, the full size geometric scale results in a higher level of explosion. The parameters discussed here need to be incorporated in the design of safety equipment.

A number of factors affect achieving DDT in smooth tubes. While the tube diameter, length and its geometry are important, the volume of combustible material and the energy of the ignition source also play vital roles in the explosion activities. The length to diameter ratio of a smooth tube is required to be higher than 70 to achieve DDT from methane–air mixture in smooth tubes.

Obstacles and geometries are crucial in transforming a deflagration flame to devastating detonation explosion. The effects of obstacles such as Schelkin spiral and orifice plates have been discussed. In an actual coal mine scenario, a number of obstacles can be noted including rubbles, buildings, vehicles, pipes and machineries. The shapes of these obstacles are diverse and have potential to accelerate DDT. Caution is therefore required to develop a valid safety strategy. Awareness of potential hazards resulting from deflagration and detonations are important and specialised safety devices should be utilised to prevent DDT of explosions.

Acknowledgement

This work was supported by the Department of Resources Energy and Tourism, Australia (grant number – G1201029) and ACA Low Emissions Technologies Ltd., Australia (grant number – G1400523).

References

AFMFI, 1940. The associated factory Mutual Fire Insurance Companies, properties of flammable liquids, gases, and solids. Ind. Eng. Chem. 32, 880–884.
Ajrash, M.J., Zanganeh, J., Moghtaderi, B., 2016a. Effects of ignition energy on fire and explosion characteristics of dilute hybrid fuel in ventilation air methane. J. Loss Prev. Process Ind. 40, 207–216.
Ajrash, M.J., Zanganeh, J., Moghtaderi, B., 2016b. Methane-coal dust hybrid fuel explosion properties in a large scale cylindrical explosion chamber. J. Loss Prev. Process Ind. 40, 317–328.
Andersson, B., Holmstedt, G., Dagneryd, A., 2003. Determination of the equivalence ratio during fire, comparison of techniques. Fire Saf. Sci. 7, 295–308.
Ashman, L., Büchler, A., 1961. The ignition of gases by electrically heated wires. Combust. Flame 5, 113–121.
Baker, W.E., Cox, P., Kulesz, J., Strehlow, R., Westine, P., 2012. Explosion Hazards and Evaluation. Elsevier.
Bartknecht, W., 1993. Explosionsschutz, Grundlagen und Anwendung. Springer Verlag, Berlin, Heidelberg, New York.
Bozier, O., Sorin, R., Virot, F., Zitoun, R., Desbordes, D., 2009. Detonability of binary H_2/CH_4–air mixtures. In: Proceedings of Third ICHS, ID 188.
Brown, M., 2010. Australia's Worst Disasters (Hachette UK).
Bull, D., Elsworth, J., Quinn, C., Hooper, G., 1976. A study of spherical detonation in mixtures of methane and oxygen diluted by nitrogen. J. Phys. D Appl. Phys. 9, 1991.
Bunev, V., Bolshova, T., Babkin, V., 2013. The nature of the upper laminar flammability limit in methane-air mixtures at high pressures. Dokl. Phys. Chem. 197–199.
Bunte, K., Bloch, A., 1935. Ignition temperatures of gases. Gas- Wasserfachm. 20, 349.
Carroll, E., "NFPA 67 ROP TC Letter Ballot (F2012) " (NFPA website, https://www.nfpa.org/Assets/files/AboutTheCodes/67/67_F2012_ROP_ballot.pdf) (accessed: 15 10 15.).
Chan, C., Moen, I., Lee, J., 1983. Influence of confinement on flame acceleration due to repeated obstacles. Combust. Flame 49, 27–39.
Chapman, D.L., 1899. On the rate of explosion in gases. Lond. Edinb. Dublin Philos. Mag. J. Sci. 47, 90–104.
Checkel, M.D., Ting, D.S.-K., Bushe, W.K., 1995. Flammability limits and burning velocities of ammonia/nitric oxide mixtures. J. Loss Prev. Process Ind. 8, 215–220.
Chen, J.R., Tsai, H.Y., Chien, J.H., Pan, H.J., 2011. Flow and flame visualization near the upper flammability limits of methane/air and propane/air mixtures at elevated pressures. J. Loss Prev. Process Ind. 24, 662–670.
Cheremisinoff, N.P., 2013. Industrial Gas Flaring Practices. Scrivener Publishing LLC., Beverly, MA.
Ciccarelli, G., Johansen, C.T., Parravani, M., 2010. The role of shock–flame interactions on flame acceleration in an obstacle laden channel. Combust. Flame 157, 2125–2136.
Claessen, G., Vliegen, J., Joosten, G., Geersen, T., 1986. Flammability characteristics of natural gases in air at elevated pressures and temperatures. In: Proc. 5th Ed., Int. Symp. Loss Prevention and Safety Promotion in the Process Industries, Cannes (F).
Coward, H., 1934. Ignition temperatures of gases."Concentric tube" experiments of (the late) Harold Baily Dixon. J. Chem. Soc. (Resum.) 1382–1406.
De Rosa, M.I., 2004. Analysis of Mine Fires for All US Underground and Surface Coal Mining Categories: 1990-1999. US Department of Health and Human Services, Public Health Service, Centers for Disease Control and Prevention, National Institute for Occupational Safety and Health, Pittsburgh Research Laboratory.
Dhillon, B., 2010a. Global mine accidents. Mine Saf. A Mod. Approach 59–71.
Dhillon, B.S., 2010b. Mine safety: a modern approach. Springer Science & Business Media.
Dingsdag, D., 1993. The Bulli Mining Disaster 1887: Lessons from the Past. St Louis Press, Darling Heights.
Dorofeev, S., Efimenko, A., Kochurko, A., 1992. Evaluation of Worst-case Loads to Reactor Containment from Fast Hydrogen Combustion. Report RRC. Kurchatov Institute.
Dorofeev, S., Kochurko, A., Efimenko, A., Chaivanov, B., 1994. Evaluation of the hydrogen explosion hazard. Nucl. Eng. Des. 148, 305–316.
Dorofeev, S., Sidorov, V., Dvoinishnikov, A., Breitung, W., 1996. Deflagration to detonation transition in large confined volume of lean hydrogen-air mixtures. Combust. Flame 104, 95–110.
Dorofeev, S., Sidorov, V., Kuznetsov, M., Matsukov, I., Alekseev, V., 2000. Effect of scale on the onset of detonations. Shock Waves 10, 137–149.
Eckhoff, R., 2005. Explosion Hazards in the Process Industries. Gulf Publishing Company, Houston, Texax.
Eckhoff, R.K., Thomassen, O., 1994. Possible sources of ignition of potential explosive gas atmospheres on offshore process installations. J. Loss Prev. Process Ind. 7, 281–294.
Fenstermaker, R., 1982. Study of autoignition for low pressure fuel—gas blends helps promote safety. Oil Gas J. 80, 126–129.
Fitch, E.C., 1992. Proactive Maintenance for Mechanical Systems. Elsevier Science Publishers Ltd., England.
Freyer, F., Meyer, V., 1893. On the ignition temperatures of explosive gas mixtures. Z. Phys. Chem. 11, 28.
Frolov, S., 2008. Fast deflagration-to-detonation transition. Russ. J. Phys. Chem. B 2, 442–455.
Frolov, S.M., Aksenov, V.S., 2007. Deflagration-to-detonation Transition in a Kerosene-air Mixture, Doklady Physical Chemistry. Springer, pp. 261–264.
Gamezo, V.N., Ogawa, T., Oran, E.S., 2008. Flame acceleration and DDT in channels with obstacles: effect of obstacle spacing. Combust. Flame 155, 302–315.
Gamezo, V.N., Zipf, R.K., Sapko, M.J., Marchewka, W.P., Mohamed, K.M., Oran, E.S., Kessler, D.A., Weiss, E.S., Addis, J.D., Karnack, F.A., 2012. Detonability of natural gas–air mixtures. Combust. Flame 159, 870–881.
Gavrikov, A., Efimenko, A., Dorofeev, S., 1999. Detonation cell sizes from detailed chemical kinetic calculations. In: 17th International Colloquium on the Dynamics of Explosions and Reactive Systems, Heidelberg, Germany.
Gavrikov, A., Efimenko, A., Dorofeev, S., 2000. A model for detonation cell size prediction from chemical kinetics. Combust. Flame 120, 19–33.
Gelfand, B., Bartenev, A., Frolov, S., Tsyganov, S., 1993. Thermal detonation in molten Sn-water suspension. Prog. Astronaut. Aeronaut. 154, 459–473.
Gharagheizi, F., 2008. Quantitative structure– property relationship for prediction of the lower flammability limit of pure compounds. Energy Fuels 22, 3037–3039.
Gieras, M., Klemens, R., Rarata, G., Wolański, P., 2006. Determination of explosion parameters of methane-air mixtures in the chamber of 40 dm^3 at normal and elevated temperature. J. Loss Prev. Process Ind. 19, 263–270.
Goethals, M., Vanderstraeten, B., Berghmans, J., De Smedt, G., Vliegen, S., Van't Oost, E., 1999. Experimental study of the flammability limits of toluene–air mixtures at elevated pressure and temperature. J. Hazard. Mater. 70, 93–104.
Guirao, C., Knystautas, R., Lee, J., 1989. A Summary of Hydrogen-air Detonation Experiments. Division of Systems Research, Office of Nuclear Regulatory Research, US Nuclear Regulatory Commission.
Hartman, H.L., Mutmansky, J.M., Ramani, R.V., Wang, Y., 2012. Mine Ventilation and Air Conditioning. John Wiley & Sons.
Ibrahim, S., Masri, A., 2001. The effects of obstructions on overpressure resulting from premixed flame deflagration. J. Loss Prev. Process Ind. 14, 213–221.
James, H., "Basic Phenomenology of Deflagration, DDT and Detonation" (UKELG website, http://ukelg.ps.ic.ac.uk/41HJ1.pdf) (accessed: 09 09 15.).

Johansen, C.T., Ciccarelli, G., 2009. Visualization of the unburned gas flow field ahead of an accelerating flame in an obstructed square channel. Combust. Flame 156, 405–416.
Jouguet, J.C.E., 1905. Sur la propagation des réactions chimiques dans les gaz. J. Math. Pures Appl. 1, 347–425.
Kessler, D., Gamezo, V., Oran, E., 2010. Simulations of flame acceleration and deflagration-to-detonation transitions in methane–air systems. Combust. Flame 157, 2063–2077.
Khanna, V.K., 2001. A Study of the Dynamics of Laminar and Turbulent Fully and Partially Premixed Flames. Mechanical Engineering. Virginia Polytechnic Institute and State University, Blacksburg, VA, USA, pp. 10–10.
Kindracki, J., Kobiera, A., Rarata, G., Wolanski, P., 2007. Influence of ignition position and obstacles on explosion development in methane–air mixture in closed vessels. J. Loss Prev. Process Ind. 20, 551–561.
King, R., 1990. Safety in the Process Industries. Butterworth-Heinemann Ltd.
Kogarko, S., 1958. Detonation of methane-air mixtures and the detonation limits of hydrocarbon-air mixtures in a large-diameter pipe. Sov. Phy. Tech. Phys. 3, 1904–1916.
Kuchta, J.M., 1985. Investigation of fire and explosion accidents in the chemical, mining, and fuel-related industries. U. S. Dep. Inter. Bureau Mines 680, 9–13.
Kuznetsov, M., Ciccarelli, G., Dorofeev, S., Alekseev, V., Yankin, Y., Kim, T., 2002. DDT in methane-air mixtures. Shock Waves 12, 215–220.
Landau, L.D., Lifshitz, E.M., 1987. Fluid Mechanics. Course on Theoretical Physics, , second ed.vol. 6. Butterwork-Heinemann, Oxford, U.K.
Lee, H., 2003. A Reflection on the Mt Kembla Disaster, 3. Illawarra Unity-Journal of the Illawarra Branch of the Australian Society for the Study of Labour History, pp. 33–45.
Lee, J., Knystautas, R., Chan, C., 1985. Turbulent Flame Propagation in Obstacle-filled Tubes, Symposium (International) on Combustion. Elsevier, pp. 1663–1672.
Lee, J.H., 1984a. Dynamic parameters of gaseous detonations. Annu. Rev. Fluid Mech. 16, 311–336.
Lee, J.H., Knystautas, R., Freiman, A., 1984. High speed turbulent deflagrations and transition to detonation in H_2-air mixtures. Combust. Flame 56, 227–239.
Lee, J.H.S., 1984b. In: Proc. Meeting at OYEZ Sci. And Tech. Services Ltd., London.
Li, D., Chen, X., Zhang, Y., Rangwala, A., 2015. Premixed CH_4-air flame structure characteristic and flow behavior induced by obstacle in an open duct. Adv. Mech. Eng. 7, 248279.
Liberman, M.A., 2008. Introduction to physics and chemistry of combustion: explosion, flame, detonation. Springer-Verlag Berlin Heidelberg.
Lindstedt, R., Michels, H., 1989. Deflagration to detonation transitions and strong deflagrations in alkane and alkene air mixtures. Combust. Flame 76, 169–181.
Lu, F., Meyers, J., Wilson, D., 2005. Experimental Study of a Pulse Detonation Rocket with Shchelkin Spiral, Shock Waves. Springer, pp. 825–830.
Marinović, N., 1990. Electrotechnology in Mining. Elsevier, New York, USA.
Markham, C.W., 1993. Mines Rescue Bill. https://www.parliament.nsw.gov.au/prod/parlment/hansart.nsf/V3Key/LA19940412038 (accessed 27 01 16.).
Matsui, H., 2002. Detonation propagation limits in homogeneous and heterogeneous systems. J. Phys. IV (Proc.). EDP Sci. 11–17.
Moen, I., Donato, M., Knystautas, R., Lee, J., 1980. Flame acceleration due to turbulence produced by obstacles. Combust. Flame 39, 21–32.
Moen, I., Lee, J., Hjertager, B.H., Fuhre, K., Eckhoff, R., 1982. Pressure development due to turbulent flame propagation in large-scale methane-air explosions. Combust. Flame 47, 31–52.
Naylor, C.A., Wheeler, R.V., 1931. The ignition of gases. Part VI. Ignition by a heated surface. Mixtures of methane with oxygen and nitrogen, argon, or helium. J. Chem. Soc. 2456–2467.
Nicholls, J., Sichel, M., Gabrijel, Z., Oza, R., Vandermolen, R., 1979. Detonability of Unconfined Natural Gas-air Clouds, Symposium (International) on Combustion. Elsevier, pp. 1223–1234.
Oran, E., Gamezo, V., Zipf Jr., R., 2015. Large-scale experiments and absolute detonability of methane/air mixtures. Combust. Sci. Technol. 187, 324–341.
Organ, M.K., 1987. Bulli Mine disaster centenary. Illawarra Hist. Soc. Bull. 54–56.
Pan, Y., Jiang, J., Wang, R., Cao, H., 2008. Advantages of support vector machine in QSPR studies for predicting auto-ignition temperatures of organic compounds. Chemom. Intell. Lab. Syst. 92, 169–178.
Park, D.J., Green, A.R., Lee, Y.S., Chen, Y.C., 2007. Experimental studies on interactions between a freely propagating flame and single obstacles in a rectangular confinement. Combust. Flame 150, 27–39.
Parnarouskis, M., Lind, C., Raj, P., Cece, J., 1980. Vapor cloud explosion study. In: Sixth International Conference on Liquefied Natural Gas Held at the International Conference Hall, Kyoto, Japan, April 7-10, 1980; Volume 2 of 2, Sessions 3 and 4.
Peraldi, O., Knystautas, R., Lee, J., 1986. Criteria for transition to detonation in tubes, 21st symposium (International) on combustion. Combust. Inst. 1629–1637.
Perry, R.W., Kantrowitz, A., 1951. The production and stability of converging shock waves. J. Appl. Phys. 22, 878–886.
Phylaktou, H., Andrews, G., 1991. The acceleration of flame propagation in a tube by an obstacle. Combust. Flame 85, 363–379.
Radford, J., 2014. What Happened Tragic Day of Mt Kembla Mine Disaster. Illawarra Mercury website. http://www.illawarramercury.com.au/story/2441786/what-happened-tragic-day-of-mt-kembla-mine-disaster/. accessed: 14 08 15.
Robinson, C., Smith, D., 1984. The auto-ignition temperature of methane. J. Hazard. Mater. 8, 199–203.
Salzano, E., Marra, F., Russo, G., Lee, J., 2002. Numerical simulation of turbulent gas flames in tubes. J. Hazard. Mater. 95, 233–247.
Shchelkin, K.I., Troshin, Y.K., 1964. Gasdynamics of Combustion. National Aeronautics and Space Administration.
Sorin, R., Zitoun, R., Desbordes, D., 2006. Optimization of the deflagration to detonation transition: reduction of length and time of transition. Shock Wasves 15, 137–145.
Suzuki, Y., Sarachik, M., Chudnovsky, E., McHugh, S., Gonzalez-Rubio, R., Avraham, N., Myasoedov, Y., Zeldov, E., Shtrikman, H., Chakov, N., 2005. Propagation of avalanches in Mn 12-Acetate: magnetic deflagration. Phys. Rev. Lett. 95, 147201.
Taffenel, J., 1913. Combustion of gaseous mixtures, and kindling temperatures. Comptes Rendus 157, 469.
Takita, K., Niioka, T., 1996. On detonation behavior of mixed fuels. Shock Waves 6, 61–66.
Thakur, P.C., 2006. Coal seam degasification. In: Kissell, F.N. (Ed.), Handbook for Methane Control in Mining. National Institute for Occupational Safety and Health. Pittsburgh Research Laboratory, Pittsburgh, PA, USA.
Townend, D., Chamberlain, E., 1936. The influence of pressure on the spontaneous ignition of inflammable gas-air mixtures. IV. Methane-, ethane-, and propane-air mixtures. Proc. R. Soc. Lond. Ser. A, Math. Phys. Sci. 154, 95–112.
Tsuboi, T., Nakamura, S., Ishii, K., Suzuki, M., 2009. Availability of the Imploding Technique as an Igniter for Large-scale Natural-gas-engines, Shock Waves. Springer, pp. 439–444..
Tu, J., 2011. Industrial Organization of the Chinese Coal Industry. Freeman Spogli Institute for International Studies.
Vanderstraeten, B., Tuerlinckx, D., Berghmans, J., Vliegen, S., Van't Oost, E., Smit, B., 1997. Experimental study of the pressure and temperature dependence on the upper flammability limit of methane/air mixtures. J. Hazard. Mater. 56, 237–246.
Wolański, P., Kauffman, C., Sichel, M., Nicholls, J., 1981. Detonation of Methane-air Mixtures, Symposium (International) on Combustion. Elsevier, pp. 1651–1660.
Yi, Y., Xueqiu, H., Geng, L., Huia, W., 2011. Effect of meshy obstacle on methane gas explosion. Proc. Eng. 26, 70–74.
Zel'dovich, Y.B., Gel'fand, B., Kazhdan, Y.M., Frolov, S., 1987. Detonation propagation in a rough tube taking account of deceleration and heat transfer. Combust. Explos. Shock Waves 23, 342–349.
Zhang, B., Bai, C., Xiu, G., Liu, Q., Gong, G., 2014. Explosion and flame characteristics of methane/air mixtures in a large-scale vessel. Process Saf. Prog. 33, 362–368.
Zhang, Q., Pang, L., Liang, H., 2011a. Effect of scale on the explosion of methane in air and its shockwave. J. Loss Prev. Process Ind. 24, 43–48.
Zhang, Q., Pang, L., Zhang, S., 2011b. Effect of scale on flame speeds of methane–air. J. Loss Prev. Process Ind. 24, 705–712.
Zhiming, Q.U., 2010. Numerical study on shock wave propagation with obstacles during methane explosion. Appl. Mech. Mater. Trans Tech Publ. 114–118.
Zipf, R.K., Gamezo, V., Sapko, M., Marchewka, W., Mohamed, K., Oran, E., Kessler, D., Weiss, E., Addis, J., Karnack, F., 2013. Methane–air detonation experiments at NIOSH Lake Lynn Laboratory. J. Loss Prev. Process Ind. 26, 295–301.
Zipf, R.K., Gamezo, V.N., Mohamed, K.M., Oran, E.S., Kessler, D.A., 2014. Deflagration-to-detonation transition in natural gas–air mixtures. Combust. Flame 161, 2165–2176.